



2nd Conference on Sustainability in Process Industry (SPI 2014) 22nd May 2014

Conference
Proceedings

www.uetpeshawar.edu.pk/spi/index.html

2nd CONFERENCE ON
SUSTAINABILITY IN PROCESS
INDUSTRY
(SPI-2014)

22nd MAY, 2014

Sponsors: PASTIC NAFS Technology LINKS

Visit on: <http://www.nwfpuet.edu.pk>

Department of Chemical Engineering UET Peshawar

SPI^{2nd} - 2014
Sustainability in Process Industry

CONFERENCE PROCEEDINGS



EDITORIAL BOARD

Dr. Saeed Gul

Dr. Mohammad Younas

Dr. Muddasar Habib

Dr. Jamil Ahmad

Dr. M. Imran Ahmad

Dr. Irshad Ali

Engr. Mansoor Ul Hasan

Engr. Quratul Ain



ORGANIZING COMMITTEE

Conference Patron

Engr. SyedImtiaz Hussain Gilani

Vice Chancellor

Conference Advisor

Prof. Dr. Zahid Mahmood

Dean Faculty of Engineering

Conference Chair

Dr. Saeed Gul

Conference Co-Chair

Dr. Mohammad Younas

Conference Secretary

Dr. Muddasar Habib

Finance Secretary

Dr. Mohammad Younas

Protocol and Registration Committee

Engr. Imran Khan Swati

Engr. Muhammad Irfan



SCIENTIFIC EXPERT COMMITTEE

Prof.Dr. Shahid Naveed (UET Lahore)

Prof. Dr. Zafar Noon (UET Lahore)

Prof. Dr. Mehmood Saleem (ICET University)

Prof. Dr. Shahid Raza Malik (NFC Faisalabad)

Prof. Dr. Sohail A Soomro (MUET Jamshoro)

Prof. Dr. Arshad Hussain (NUST Islamabad)

Prof. Dr. Suleman Tahir (University of Gujrat)

Prof. Dr. Naveed Ramzan (UET Lahore)

Prof. Dr. Sahar Noor (UET Peshawar)

Dr. Saeed Gul (UET Peshawar)

Dr. Mohammad Younas (UET Peshawar)



ACKNOWLEDGEMENT

It is our great pleasure to welcome you to the SPI-2014 conference on “**Sustainability in Process Industry (SPI-2014)**”. Putting together SPI-2014 was a team effort. We first thank the authors for providing the content of the program in the form of oral and poster presentations and all other participants. We are also grateful to the key note speakers from academia and various industries. These valuable and insightful talks can and will guide us to a better understanding of the “**Sustainability in Process Industry**”.

We also thank the hosting organization, UET, Peshawar, and our generous sponsors PASTIC, NAYS. Technology Links (pvt) Ltd. And Rizvi and Co. (pvt) Ltd. without their great support it would not be possible to hold this conference. The support and funding they provided is greatly appreciated.

We are grateful to the program committee, who worked very hard in order to make this conference successful.



SPONSOR PROFILE

PASTIC

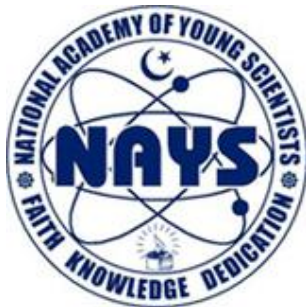


PASTIC is the premier organization for dissemination of Scientific and Technological Information to the Scientists, Researchers, Engineers, Entrepreneurs, Industry and Citizens of Pakistan. PASTIC National Center is located in Quaid-e-Azam University Campus in Islamabad. It has six Sub Centers throughout Pakistan including Karachi, Lahore, Peshawar, Quetta, Faisalabad and Muzaffarabad. PASTIC's services include Bibliographic Service, Document Supply Service, Abstracting and Indexing Service, National Science Reference Library, Repographic Services, and Technology Information Services. PASTIC works under Pakistan Science Foundation which is the public organization for the promotion of Scientific Activities across Pakistan.

PASTIC National Centre, QAU Campus, Islamabad.

Ph# 051-9248103-04

NAYS



NAYS is the torchbearer in mobilizing young scientists (researchers/professionals) and scholars at a platform by providing them an environment where they can collaborate and exchange their fruitful innovative ideas and information in multidisciplinary science domains with an advisor council that includes crew of highly qualified professors for their guidance. It is helpful for young researchers for further research, to enrich their knowledge and to prove their flair in research oriented subjects. Moreover, NAYS firmly believes that engaging young scientists (researchers / professionals) and utilizing their capabilities by better orientation, improvisation and execution would definitely bring a remarkable boom of science and technology in Pakistan.



Your connection to the Future.

The company specializes in the supply, installation and maintenance of equipment in the fields of Education, Training, Research, Quality Control, Laboratory, Health, Environment & Pollution Control, and Material Testing.

Head Office (Karachi)

Technology Links (Pvt) Limited
4-10/11, Rimpa Plaza, M. A. Jinnah Road, Karachi-Pakistan
Phone: +92-21-32734260- 61
Fax: +92-21-32730728
Email: info@technologylinks.com.pk



www.technologylinks.com.pk



RIZVI & Company



B-24, Block-9, Gulshan-e-Iqbal
P. O. Box No. 17514,
KARACHI-75300
Ph. No. (021) 34827124 – 34821116
Fax No. (92-21) 34968626 – 34993570
E-mail: sales@rizviandco.com.pk



PREFACE

Sustainability means “to maintain or endure.” According to the work of the UN Brundtland Commission, sustainability in the context of development is to “meet the needs of the present without compromising the ability of future generations to meet their own needs.” The sustainability in process industries has globally known from the last few decades. Sustainable development contains social, cultural, environmental and economic aspects. The country like Pakistan is facing various problems and energy is one of the main issues today. There are many reasons of energy crises in Pakistan and non- sustainable process is one of the major factors among them. This is the right time to address the sustainability and link it to the process industries to be sustainable and contribute to sustainable development in order to overcome the energy crises in Pakistan.

The Chemical Engineering Department of University of Engineering and Technology, Peshawar plays a crucial role in research areas of national interest. Our faculty is energetically involved in applied research at both national and international level.

The 1st conference on “**Sustainability in Process Industries (SPI-2012)**”, held at UET, Peshawar on August 10, 2012, attracted prominent researchers from all over Pakistan which created a linkage and provided approaches to the application of sustainability in the process industry.

Continuing the same tradition, the Department of Chemical Engineering had again taken initiative to hold a 2nd conference on “**Sustainability in Process Industries (SPI-2014)**”, on May 22, 2014 in collaboration with PASTIC and NAYS. The mission of the conference is to share and identify new directions for future research and development regarding “**Sustainability in Process Industries**”.

We hope that you will find this program interesting and that the conference will provide you with a valuable opportunity to share ideas with other researchers.

Organizing Committee



TABLE OF CONTENTS

EDITORIAL BOARD	ii
ORGANIZING COMMITTEE	iii
SCIENTIFIC EXPERT COMMITTEE	iv
ACKNOWLEDGEMENT	v
SPONSOR PROFILE	vi
PREFACE	ix
TABLE OF CONTENTS	x
CFD Simulation of Non-Dispersive Solvent Extraction in Membrane Contactors	
Amir Muhammad, Mohammad Younas	1
Numerical Solution of Highly Oscillatory Fredholm Integral Equation – A Mesh free Approach	
Zaheer-ud-Din , Siraj-ul-Islam	6
Numerical Solution of SIR Model by Meshless and Finite Difference Methods	
Saeed Ullah Jan, Siraj-Ul-Islam.....	12
Cost Effective Approach for Risk Analysis of Natural Gas Pipelines	
Muhammad Noman Saeed Gul.....	18
Numerical simulation of pure diffusion model by Haar wavelets	
Muhammad Ahsan, Siraj-Ul-Islam	23
Numerical Solution Method of Highly Oscillatory 1D Fredholm Integral Equation	
Tariq Mahmood, Siraj-ul-Islam	28
Effect Of CO ₂ On The Growth Rate of Microalgae in a Photo Bioreactor (Pbr)	
Asmatullah,Mohammad Younas.....	34
Solving two-dimensional Poisson equation with nonlocal boundary conditions by meshless method	
Masood Ahmad, Siraj-u-islam	39
Review of Process Simulation and Simulation Software-Open Source Software Development	
Muhammad Shoaib, Walter Wukovits, Saeed Gul	45
Meshless based complex quadrature solution for highly oscillatory integrals and the integrals having no stationary points	
Uzma Nasib, Siraj-ul-Islam	50
Modeling and Simulation of Osmotic Distillation Process of Fruit Juice Concentration	
Sher Ahmad, Dr. Muhammad Younas.....	56
Simulation of HFMC for Heavy Metal (Cu) Extraction With Chelating Extractants	
Iftikhar Ahmed, Dr. Muhammad Younas	63



Conference Proceedings SPI 2014 [1-5]

CFD Simulation of Non-Dispersive Solvent Extraction in Membrane Contactors

Amir Muhammad¹, Mohammad Younas²

^{1,2} Department of Chemical Engineering, University of Engineering & Technology, Peshawar, Pakistan,
PO Box 814, Post code 25120

¹engr_amir14@yahoo.com, ²engr_unas@nwfpuet.edu.pk

Abstract:

In this study is presented a 2-D axial-radial steady-state numerical model for dispersion free liquid-liquid extraction in a hollow fiber membrane contactor. Axial-radial convection and diffusion mass transfer is considered in both tube and shell sides of the contactor, while only diffusion through membrane. Momentum balance equations have been coupled with mass transfer continuity equations to study the concentration and velocity profiles across the membrane contactor, e.g. in shell and tube sides and through pores of membrane. The model equations have been solved with Computational Fluid Dynamics (CFD) techniques using finite element method in COMSOL MultiphysicsTM Software. The effects of process parameters on solute extraction efficiency of contactor have been studied and it was confirmed that these devices are efficient for solute removal under liquid-liquid extraction mode. Furthermore, it was also observed that CFD study gives a detailed and clear analysis of dispersion free liquid-liquid extraction process in membrane contactors.

Keywords: Solvent extraction, Mass transfer, Hollow fiber membrane contactors, Modeling and simulation, Computational fluid dynamics

1. Introduction

Hollow fiber membrane contactors (HFMCs) as a novel technique for liquid-liquid extraction have attracted the most attentions for the last three decades. It is due to their dispersion free contact, higher mass transfer interfacial area and compactness of the unit that overcome the drawbacks of conventional extractors. The conventional extraction units used for liquid-liquid extraction are tray columns, packed towers etc. In these units two phases i-e aqueous feed and organic solvent are brought into a direct contact for mass transfer to occur. The main purpose of these units is to maximize the interfacial area, however due to dispersive contact of phases these units suffer from a number of disadvantages like flooding, entraining, weeping and high capital and operating costs. HFMCs in comparison to conventional extractors allow two phases to come into a direct contact without dispersion of one phase into another thus avoid the disadvantages of conventional units and allow the independent control of two phases [1]. Furthermore, there is no need for a difference in phase densities thus leading to a greater choice of extracting solvents [2].

Mass transfer modeling of these membrane contactors has been remained a focus of interest for several researchers in recent years [3]. Reliable mass transfer modeling of membrane contactors is necessary to predict their performance under given conditions and for design and optimization purposes allowing to accurate scale-up processes. In present study a two dimensional axial radial mass transfer model has been developed to study the transport of copper (II) solute through a single hypothesized "flow-cell", adapted from the previous study for the baffle less hollow fiber membrane contactor module for liquid-liquid extraction [4]. The flow-cell consists of three

sections i-e tube side, inside membrane and shell side. Aqueous feed that contains the solute flows in tube side while organic solvent flows in shell.

The aim of this work is to study the distribution of copper in three sections of flow-cell through mathematical modelling and CFD simulation. Other interests of the study are to identify the different regions of velocity profile in shell side and to find the effects of process parameters on membrane extractor performance using CFD techniques.

2. Theory

2.1 Model development

Figure 1(a) shows a single “flow-cell” configuration as modelled in previous work [21]. The identical flow-cell geometry looks like a concentric tube arrangement. Each flow-cell consists of three sections. The inner tube is the fiber side. The outer concentric tube is denoted by shell side of the membrane contactor. The third section of the assembly is the thickness of the inner tube, termed as porous membrane and is sandwiched between the two sections. The flow-cell assembly is shown in figure 1(b). The inside radius of fiber is shown by R_1 . R_2 indicates the outer side of fiber. R_3 is indicated for the radius of flow-cell while $R=0$ shows the centre of fiber. Aqueous phase that contains the copper (II) solute flows in tube side and organic phase counter currently in shell. A trans-membrane pressure is applied on aqueous side in order to prevent the organic solution to enter into aqueous phase.. This model is based on the idea that two concentric tubes are used as the model for fluid flowing out of the fibers and so only portion of fluid surrounding the fiber is considered and may be approximated as circular cross section [5]. The transfer of solute in tube side occurs through diffusion and convection mass transfer which, under steady-state conditions and with no chemical reaction, is shown by equation (1) [6].

$$-D_{i-tube} \nabla C_{i-tube} + C_{i-tube} u_{z-tube} = 0 \tag{1}$$

Where C_{i-tube} is concentration and D_{i-tube} is diffusion coefficient of solute i in tube side i-e aqueous phase and u_{z-tube} is axial velocity of aqueous phase along the length of module.

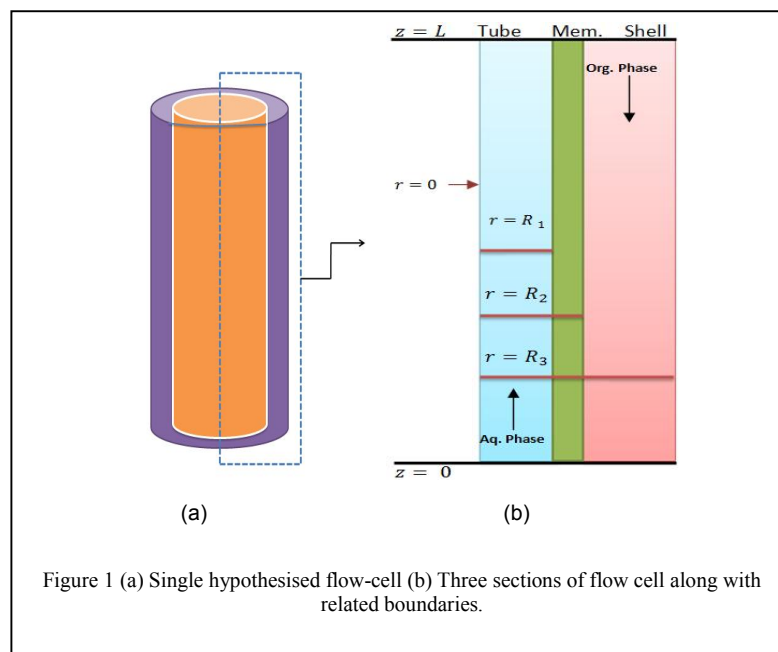


Figure 1 (a) Single hypothesised flow-cell (b) Three sections of flow cell along with related boundaries.

The flow in tube side has been assumed to be laminar and fully developed so velocity distribution of aqueous phase is given by equation (2)



$$u_{z-tube} = 2u \left[1 - \left(\frac{r}{R_1} \right)^2 \right] \quad (2)$$

The transfer of solute through the hydrophobic membrane occurs through diffusion and is given by following steady-state continuity equation.

$$-D_{i-mem} \nabla C_{i-mem} = 0 \quad (3)$$

Likewise, the solute transfer in flow-cell side through diffusion and convection mass transfer is described by following steady-state continuity equation,

$$-D_{i-fc} \nabla C_{i-fc} + C_i u_{z-fc} = 0 \quad (4)$$

Where C_{i-fc} is concentration of solute in shell side.

The equation (5) describes flow in viscous fluids through momentum balances for each of the component. The Navier-Stokes equation (5) is then coupled with continuity equation (4) to characterize the flow in flow-cell side and to find the concentration profile of solute in this region.

$$\rho u \cdot \nabla u - \nabla \cdot \mu (\nabla u + (\nabla u)^T) + \nabla p = F, \quad \nabla u = 0 \quad (5)$$

Where ρ denotes the density (kg/m^3), u the velocity vector (m/s), μ the dynamic viscosity ($kg/m.s$) p the pressure (Pa) and F the body force term (N) such as gravity.

2.2 CFD Simulation of Model Equations

The model equations with associated boundary conditions are solved with CFD techniques. For this purpose COMSOL Multiphysics software is used. COMSOL Multiphysics employs finite element method (FEM) for numerical solution of model equations. The finite element analysis is combined with adaptive meshing and error control using numerical solver of UMFPAK. The dimensions of the hollow-fiber membrane contactor and simulation parameters are listed in Table 1.

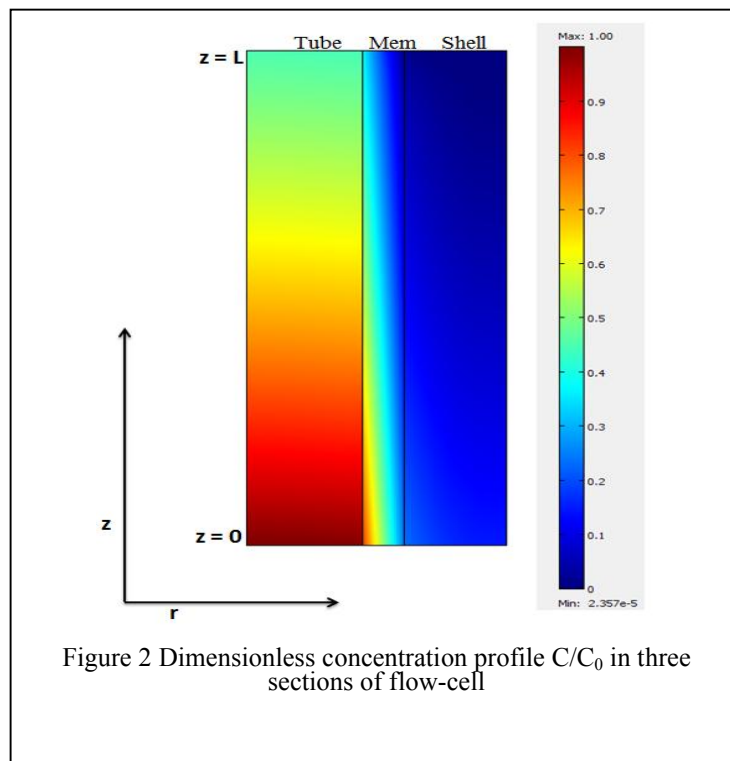
TABLE 1
Geometrical and simulation parameters of the hollow fiber membrane contactor module x-50 [4]

Symbols	Parameters	Values
R_1	Fiber inside radius	1.1e-4 m
R_2	Fiber outside radius	1.5e-4 m
R_3	Flowcell (Shell side) radius	2.47e-4 m
L	Length of the module [m]	121.8 × 10 ⁻³
ϵ	Porosity	0.4
τ	Tortuosity	1/ ϵ
N	No. of fibers	7400
D_{aq}	Aqueous side diffusion coefficient	2.79e-9 m ² /s
D_{org}	Organic side diffusion coefficient	1.23e-10 m ² /s
D_m	Membrane diffusion coefficient	$D_{org} (\epsilon/\tau)$ m ² /s
C_0	Initial concentration of feed	3.15 mol/m ³
S	Scale factor	200

3. Results and Discussions

3.1 Concentration Profile across membrane contactor

Dimensionless concentration profile C/C_0 of solute in hollow fiber membrane contactor is shown in Figure 2. Aqueous feed flows in tube side and organic solvent flows counter currently in the shell. Copper (II) solution is considered as aqueous phase while trifluoro-acetylacetone (TFA) as extractant diluted in 1-decanol was taken as organic phase. The physic-chemical and transport properties of both the phases have been assumed from previous study [4]. Feed enters at $z = 0$ with maximum solute concentration. Organic solvent enters at opposite side in shell i-e at $z = L$ with zero solute concentration. As the membrane is hydrophobic, organic solvent diffuses through membrane and immobilizes in tube side at membrane mouth due to trans-membrane pressure applied to aqueous phase. Solute moves from aqueous phase towards membrane contactor crosses the interface and reacts with organic solvent at membrane mouth and consequently an organo-metallic complex compound is formed. This reaction of the solute with the extractant is instant at the interface and is simply assumed by the partition coefficient at the interface of aqueous phase boundary layer with the membrane. The complex compound formed diffuses from membrane into shell side due to concentration gradient and then swept out by organic phase. Concentration profile as shown by Figure 2 indicates that as aqueous feed moves along membrane contactor solute concentration decreases while concentration of solute in organic phase increases along its pathway because of continuous transfer of solute from aqueous to organic phase. It is also observed from Figure 2 that fall in solute concentration in aqueous phase is higher in the start of feed line of the contactor in tube side and then decreases slowly throughout the contactor. This initial rapid fall in solute concentration is attributed due to the fact that concentration gradient is higher in the start of feed entrance to the contactor. As aqueous feed moves forward through the contactor further away from the inlet, concentration gradient decreases which in turn decreases the mass transfer across the membrane.





4. Conclusions

A 2-dimension axial radial model was developed and solved with CFD techniques. Concentration profile for solute was investigated which gives a clear snap of solute distribution in the three sections of flow-cell. Velocity profile was also found using Navier-Stokes equation, the profile shows different regions of flow i-e undeveloped, developing and fully developed flow in the shell side of contactor. The effects of feed and organic flowrates were investigated and it was found that decreasing feed flowrate increases solute removal efficiency while the organic flowrate has an opposite effect. Simulation study confirms that a mini module of hollow fiber membrane contactor of 121 mm long sufficiently extract the copper (II) up to 10 mol.m^{-3} from aqueous streams with the extractant trifluoro-acetylacetone (TFA) depending upon the process and operating conditions in once through mode.

References

- [1] A. Gabelman, S.T. Hwang. Hollow fiber membrane contactors. *J. Membrane Science* 159, 1999 pp. 61-106
- [2] M. Younas, S.D. Bocquet, J. Sanchez. Kinetic and dynamic study of liquid-liquid extraction of copper in a HFMC: experimentation, modeling, and simulation. *AIChE J* 56, 2010, pp. 1469–1480
- [3] A.K.Pabby, A. M. Sastre. State-of-the-art review on hollow fiber contactor technology and membrane-based extraction processes,” *J. Membrane Science*. 430, 2013, pp. 263–303
- [4] M. Younas, S.D. Bocquet, J. Sanchez. Experimental and theoretical mass transfer transient analysis of copper extraction using HFMCs. *J. Membrane Science* 82, 2011, pp. 70–81
- [5] M. Mahdavian, H. Atashi, M. Zivdar, M. Mousavi. Simulation of CO₂ and H₂S removal using methanol in hollow fiber membrane gas absorber (HFMDGA). *Advances in Chemical Engg. and Sciences* 2, 2012 50-61
- [6] R.B. Bird, W.E. Stewart, E.N. Lightfoot. *Transport Phenomena*. John Wiley & Sons, 1960



Conference Proceedings SPI 2014 [6-11]

Numerical Solution of Highly Oscillatory Fredholm Integral Equation – A Mesh free Approach

Zaheer-ud-Din¹, Siraj-ul-Islam²

^{1,2} Department of Basic Sciences, University of Engineering & Technology, Peshawar, Pakistan, PO Box 814, Post code 25120

¹zaheeru1977@gmail.com, ²siraj.islam@gmail.com

Abstract:

In this paper, a modified Levin's quadrature method is put forward for numerical solution of two-dimensional highly oscillatory Fredholm integral equation. The method focuses on the highly oscillatory kernel having phase function free of stationary phase points. The suggested quadrature is efficient and accurate. The Numerical examples provided at the end demonstrate its effectiveness.

Keywords: Oscillatory integral equation, Levin's quadrature, Multi Quadric Radial Basis Functions

1. Introduction

Fredholm integral equations can be obtained from boundary value problems with given boundary conditions [10]. The Fredholm integral equations are widely used in the field of Engineering and Science, especially in the field of scattering problems, optics, acoustics, quantum mechanics and electromagnetic waves etc. [1, 5]. The two-dimensional Fredholm integral equation of the second kind where the unknown function appear inside and outside of the integral sign is presented by the form:

$$\mu(x, t) = h(x, t) + \int_a^b \int_c^d k(x, t, u, z) \mu(u, v) dudv, \quad (x, t) \in [a, b] \times [c, d] \quad (1)$$

where $k(x, t, u, z)$ is the kernel function and $\mu(u, v)$ is the unknown function.

We can write the above integral equations in the oscillatory form as:

$$\mu(x, t) = h(x, t) + \int_a^b \int_c^d f(x, t, u, v) e^{i\omega g(x, t, u, v)} \mu(u, v) dudv, \quad (2)$$

which is highly oscillatory Fredholm integral equation (HOFIE) having kernel with phase function g while f, g, h and μ are considered smooth functions represent the frequency of oscillations. Increasing ω will results in highly oscillatory kernel. This is really a competitive problem which needs a special attention to handle. The literature is



inadequate on subject of solution of two-dimensional HOFIE. This area has not being watched and need attention to find efficient algorithm for numerical solution of Fredholm integral equations having highly oscillatory kernels.

Different methods [2, 11, 5, 3] in past have been developed which are primarily concerned the case where the integral equations having non-oscillatory kernel functions. Very accurate algorithm for solution of one-dimensional HOFIE has been provided by J. Li et al. [7] based on his work done for two-dimensional highly oscillatory integrals (HOIs) [6].

Recently Levin's based multi quadric RBF method have been developed by Siraj-ul-Islam et al. [8, 9] to find numerical solution of one and two-dimensional HOIs. In this study we investigate an efficient and accurate algorithm in the form of Proposed Quadrature of the Integral Equation (PQIE) based on Levin's quadrature theory involving multi quadric RBF for solving two-dimensional HOIs.

2. Proposed Quadrature of the Integral Equation

The algorithm PQIE is easy to implement. Discretizing the HOFIE (2) on the given nodes

(x_r, t_r) , $r = 1, \dots, M^2$ we have

$$\mu(x_r, t_r) = h(x_r, t_r) + \int_a^b \int_c^d f(x_r, t_r, u, v) e^{\iota \omega g(x_r, t_r, u, v)} \mu(u, v) dudv, \quad (3)$$

We need to evaluate the following HOIs;

$$I_r = \int_a^b \int_c^d f(x_r, t_r, u, v) e^{\iota \omega g(x_r, t_r, u, v)} \mu(u, v) dudv, \quad (4)$$

To get solve the above HOIs we use Levin's quadrature theory. Accordingly we need to find a suitable function $p(u, v)$ which is agreeable to the following PDE:

$$p_{yz} + \iota \omega g_v p_u + \iota \omega g_u p_v + (\iota \omega g_{yz} - \omega^2 g_v g_u) p = f(x_r, t_r, u, v) \mu(u, v) \quad (5)$$

Once the unknown function $p(u, v)$ is obtained from (5) then the integral value is found from

$$I_r = p(b, d) e^{\iota \omega g(x_r, t_r, b, d)} - p(a, d) e^{\iota \omega g(x_r, t_r, a, d)} \\ - p(b, c) e^{\iota \omega g(x_r, t_r, b, c)} + p(a, c) e^{\iota \omega g(x_r, t_r, a, c)} \quad (6)$$



In [9], multi quadric RBF method is employed to solve the PDE (5) on the regular nodes. In this technique we replace the unknown function $p(u, v)$ and its derivatives by the corresponding MQRBF approximation given by

$$p(u, v) = \sum_{l=1}^{N^2} \lambda_l \Phi(r_l) = \sum_{l=1}^{N^2} \lambda_l \sqrt{C^2 + r_l^2}, \quad (u, v) \in \Omega. \quad (7)$$

where C is the shape parameter and

$$r_l = \sqrt{(u - u_l)^2 + (v - v_l)^2},$$

λ_l are the RBF coefficients.

Using [5] and (7) with a little bit manipulation we get in matrix notation, the following numerical value of $p(u, v)$;

$$\mathbf{P}_r(\mathbf{u}, \mathbf{v}) = \mathbf{C}_r^{-1}(\text{diag}(\mathbf{F}_r)\Psi)\Phi, \quad (8)$$

where \mathbf{C}_r^{-1} is the coefficient matrix obtained from the system of linear equations after using the corresponding MQRBF and

$$\mathbf{P}_r(u, v) = [p(u_1, v_1), p(u_2, v_2), \dots, p(u_{N^2}, v_{N^2})]^T$$

$$\Psi = [\mu(u_1, v_1), \mu(u_2, v_2), \dots, \mu(u_{N^2}, v_{N^2})]^T$$

and

$$\mathbf{F}_r = [f(x_r, t_r, u_1, v_1), f(x_r, t_r, u_2, v_2), \dots, f(x_r, t_r, u_{N^2}, v_{N^2})]^T$$

represent vectors.

2.1 Free of Stationary Phase Point approach

The integral [4] is wholly dependent on the limits of integration, resulting a vector of zeros entries except the limits of integration. This vector has the form;

$$\mathbf{Q}_r = \begin{bmatrix} e^{\iota \omega g(x_r, t_r, a, c)} & \text{zeros}(1, N - 2) & -e^{\iota \omega g(x_r, t_r, b, c)} & \text{zeros}(1, N(N - 2)) \\ -e^{\iota \omega g(x_r, t_r, a, d)} & \text{zeros}(1, N - 2) & e^{\iota \omega g(x_r, t_r, b, d)} & \end{bmatrix} \quad (9)$$



Now we can write [4] using [8] and [9] in the following form

$$I_r = Q_r P_r \quad (10)$$

Let

$$V_r = Q_r C_r^{-1} (\text{diag}(F_r) \Phi) \quad (11)$$

where V_r are complex vectors of order $1 \times N^2$ then

$$I_r = V_r \Psi \quad (12)$$

where Ψ is a complex vector of order $N^2 \times 1$.

Now substituting the integral value [12] in [3] we get

$$\mu(x_r, t_r) = h(x_r, t_r) + V_r \Psi \quad (13)$$

To get the unknown Ψ we suppose a square mesh in both (x, t) and (u, v) direction i.e. $M = N$;

Hence [13] will lead us to the following linear system;

$$\Psi = H + V \Psi \quad (14)$$

Here H is a $N^2 \times 1$ vector of complex numbers where as V is of order $N^2 \times N^2$ having complex entries.

To get Ψ which is the solution of the integral equation, the last equation [14] can be transformed to

$$\Psi = (I - V)^{-1} H \quad (15)$$

which gives the required numerical solution of the HOFIE.

3. Results and Discussions

To check the accuracy of the proposed method we analyse the problems by absolute and relative errors. Whereas the value of the shape parameter is considered $C=0.5$. Absolute and relative errors are defined as follows:

$$L_{ab} = |approx - exact|$$
$$L_{\infty} = max[L_{ab}]$$
$$L_{re} = \frac{L_{ab}}{|exact|}$$



Table 1: Test Problem (1), accuracy L_∞ and L_{re} versus varying ω

PQIE		
ω	L_∞	L_{re}
10^1	$6.11244790231780 \times 10^{-05}$	$3.91965055816845 \times 10^{-04}$
10^2	$2.60051425565733 \times 10^{-06}$	$1.66759820505735 \times 10^{-05}$
10^3	$1.26856425364252 \times 10^{-08}$	$8.13475793393081 \times 10^{-08}$
10^4	$1.40369937895457 \times 10^{-11}$	$9.00131080783240 \times 10^{-11}$
10^5	$6.63358257213531 \times 10^{-15}$	$4.25215418431435 \times 10^{-14}$
10^6	$3.33066907387547 \times 10^{-16}$	$8.88178419700125 \times 10^{-16}$
10^7	$4.99600361081320 \times 10^{-16}$	$1.55431223447522 \times 10^{-15}$
10^8	$1.36002320516582 \times 10^{-15}$	$8.77076189453874 \times 10^{-15}$

4. Conclusions

A numerical method for the solution of two-dimensional Fredholm integral equation having highly oscillatory kernel is presented here. In physical applications of integral equations there is always need of having rapid and accurate algorithm for problems where the kernel function is highly oscillatory. This proposed method is accurate and fast with increasing frequency while keeping less number of nodal points.

References

- [1] K. Atkinson. The numerical solution of integral equations of the second kind. Cambridge University Press, Cambridge, 1997.
- [2] H. Guoqiang and W. Jiong. Extrapolation of nystrom solution for two dimensional nonlinear fredholm integral equations. Journal of Computational and Applied Mathematics, 134:259– 268, 2001.
- [3] D. Huybrechs. On the evaluation of highly oscillatory integrals by analytic continuation. SIAM Journal on Numerical Analysis, 44(3):1026– 1048, 2006.
- [4] A. Iserles and S. P. Norsett. Efficient quadrature of highly oscillatory integrals using derivatives. Proceedings of the Royal Society, 461:1388– 1399, 2005.
- [5] A. J. Jerri. Introduction to Integral Equations with Applications. John Wiley and Sons, INC, 1999.
- [6] J. Li, X. Wang, T. Wang, and C. Shen. Delaminating quadrature method for multidimensional highly oscillatory integrals. Applied Mathematics and Computation, 209(2):327– 338, 2009.
- [7] J. Li, X. Wang, S. Xiao, and T. Wang. A rapid solution of a kind of 1D Fredholm oscillatory integral equation. Journal of Computational and Applied Mathematics, 236:2696–2705, 2012.



- [8] Siraj-ul-Islam, A. S. Al-Fhaid, and S. Zaman. Meshless and wavelets based complex quadraturequadrature of highly oscillatory integrals and the integrals with stationary points. *Engineering Analysis with Boundary Elements*, 37:1136–1144, 2013.
- [9] Siraj-ul-Islam, I. Aziz, and W. khan. Numerical integration of multi-dimensional highly oscillatory, gentle oscillatory and non-oscillatory integrands based on wavelets and radial basis functions. *Engineering Analysis with Boundary Elements*, 36:1284–1295, 2012.
- [10] A. M. Wazwaz. *Linear and Non Linear Integral Equations: Methods and Appications*. Higher Education Press, Beijing and Springer-Verlog Berlin Heidekberg, Germany, 2011.
- [11] W. J. Xie and F. R. Lin. A fast numerical solution of two dimensional fredholm integral equations of the second kind. *Applied Mathematics and Computation*, 59:1709–1719, 2009.



Conference Proceedings SPI 2014 [12-17]

Numerical Solution of SIR Model by Meshless and Finite Difference Methods

Saeed Ullah Jan¹, Siraj-Ul-Islam²

*^{1,2}Department of Basic Sciences, University of Engineering & Technology,
Peshawar, Pakistan, PO Box 814, Post code 25120*

¹saeedjan53@gmail.com, ²siraj.ulislam@gmail.com

Abstract:

In this paper, the whooping cough (SIR) model which consists of susceptible (S), infected (I) and recovered (R) classes, is being considered along with diffusion term. Equilibrium points of the model have been determined i.e. disease free equilibrium point and endemic equilibrium and their stability has also discussed. The effect of diffusion has been studied in the model. The basic reproduction number of the model is also derived. A finite difference operating splitting, meshless operator splitting and a one step meshless explicit methods are being considered for numerical solutions of the model with diffusion (WD) and without diffusion (WOD). As the exact solution is not available, the numerical outputs obtained are mutually compared and their correctness is being verified by the theoretical outputs as well.

Keywords: *Meshless methods, Finite difference methods, Radial basis functions, Systems of PDEs, whooping cough.*

1. Introduction

The whooping cough is also called pertussis, is a very contagious bacterial disease caused by bacterium *Bordetella pertussis*. In some countries, this bacterial contagious disease is called cough of 100 days [3]. Whooping cough is an intensely infectious disease which is spread from person to person through contact and cause extensively fatal ailment. This is an essential subject for research in order to overcome its adverse impacts around the globe in both developed and underdeveloped countries. Because of its contagious and serious nature, pertussis erupts in epidemic waves, its outbreaks has severely risen from the last few decades [5].

Pertussis which has been a major cause of mortality in infants, has hit approximately 600,000 infants death annually around the globe [1]. Pertussis is widely found in adult and adolescents. Pertussis spread through air from the infected people mucous membranes, which is more lethal during the catarrhal stage [8]. It is because, that during the catarrhal stage its symptoms are nonspecific, it can only be diagnosed by the appearance of the symptoms of cough of the paroxysmal stage. In order to control this disease the whole-cell pertussis vaccines is used, but it cannot completely eliminated *Bordetella Pertussis* circulation [4]. The dynamics of whooping cough in population is studied here through SIR mathematical model to describe the dynamics of whooping cough epidemics using periodic variations in susceptibility [2].

A vaccination known as "DTaP" (Diphtheria, Tetanus, acellular Pertussis), which has shown quite enough resistance to this disease, but it is not 100 percent effective. The outbreaks of pertussis has commonly observed in hospitals, schools and other institutions, where the effectiveness of initial DTaP vaccine has faded away in adults and older students [5]. Different theories are present in epidemic literature, for instance, theory of "herd immunity"



and theory of "prevalence elasticity" for the eradication of this contagious disease which is commonly known as whooping cough [5].

In this paper, our focus is on the numerical simulation of the SIR model by three types of numerical methods. They include explicit meshless method (EMM), operator splitting meshless method (OSMM) and operator splitting finite difference method (OSFDM). This helps us to analyze the disease dynamics in a better way.

2. The SIR model in ODEs form

The SIR model with three Classes in ODEs form is given by

$$\begin{aligned}\frac{dS}{dt} &= \mu - \mu S - N\beta SI \\ \frac{dI}{dt} &= N\beta SI - \mu I - \nu I \\ \frac{dR}{dt} &= \nu I - \mu R\end{aligned}\quad (1)$$

with the following condition

$$S+I+R=1 \quad (2)$$

The parameters values are given in the Table. 1

Table 1: Model parameters and their values

Parameters	Value	Reference
μ	0.04	[7]
ν	24	[7]
β	123	[7]
—	223	[7]

3. The SIR model with diffusion

In the case when diffusion is added, the ODE model (1) is converted into a system of PDEs which is given by;



$$\begin{aligned}\frac{dS}{dt} &= \mu - \mu S - N\beta SI + \alpha \frac{\partial^2 S}{\partial x^2} \\ \frac{dI}{dt} &= N\beta SI - \mu I - \nu I + \alpha \frac{\partial^2 I}{\partial x^2} \\ \frac{dR}{dt} &= \nu I - \mu R + \alpha \frac{\partial^2 R}{\partial x^2}\end{aligned}\quad (3)$$

where α is diffusivity constant of susceptible (S), infected (I) and recovered (R) classes of the population. The interval $[0, 0.25]$ is being considered to be domain for SIR model. The following equations are taken as Neumann boundary conditions for the SIR model:

$$\frac{\partial \zeta(0, t)}{\partial x} = 0,$$

and

$$\frac{\partial \zeta(0.25, t)}{\partial x} = 0, \quad (4)$$

Where $\zeta = S, I, R$

4. Derivation of basic reproduction number

Basic reproduction number (BRN) R_0 [6] measures the spread of infection caused by one infected person due to which the disease spread among the population. The value of R_0 for the system Eq. (1) can be calculated as follow, we choose the matrices F and V such that

$$F = \begin{pmatrix} 0 \\ N\beta SI \\ 0 \end{pmatrix}, \quad V = \begin{pmatrix} \mu S + N\beta SI - \mu \\ \mu I + \nu I \\ \mu R - \nu I \end{pmatrix}.$$

The infected compartment is I.

Thus

$$F = (N\beta S), \quad V = (\mu + \nu).$$



The required basic reproduction number R_0 , is the eigenvalue of FV^{-1} given by,

$$R_0 = \frac{N\beta}{\mu + \nu} \quad (5)$$

5. Initial condition

The initial conditions (6) and (7) are being used for SIR model to test the effectiveness of EMM, OSMM and OSFDM. These conditions are given as:

ICs (1)

$$\begin{aligned} S_0 &= 0.24, & 0 \leq x \leq 0.25, \\ I_0 &= 0.007, & 0 \leq x \leq 0.25, \\ R_0 &= 0.753, & 0 \leq x \leq 0.25, \end{aligned} \quad (6)$$

ICs (2)

$$\begin{aligned} S_0 &= \exp(-10(x)^2) * 0.96, & 0 \leq x \leq 0.25, \\ I_0 &= \exp(-100(x)^2) * 0.04, & 0 \leq x \leq 0.25, \\ R_0 &= 0, & 0 \leq x \leq 0.25, \end{aligned} \quad (7)$$

6. Numerical Scheme

In this section, we use OSFDM, EMM and the OSMM for the numerical solution of the model given in Eq. (3). In each case, spatial step $\Delta x = 0.05$ and time step $\Delta t = 0.001$ days are used keeping in view the Von Neumann analysis for stability. The diffusivity constant value used in both the cases is $\alpha = 0.1$.

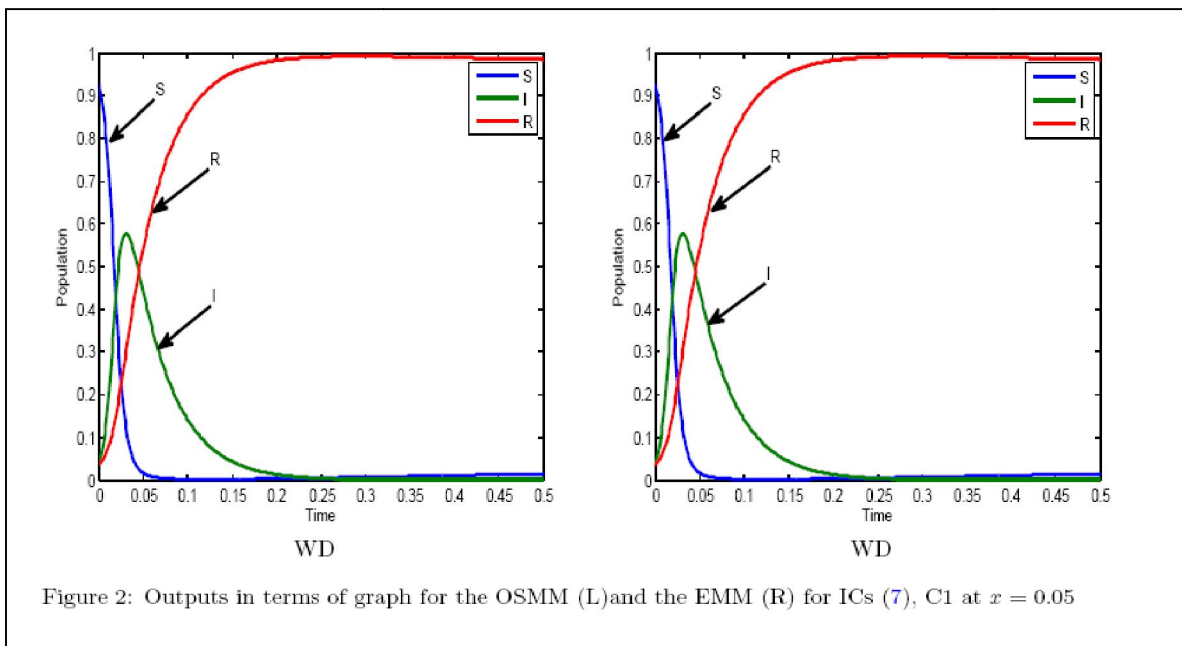
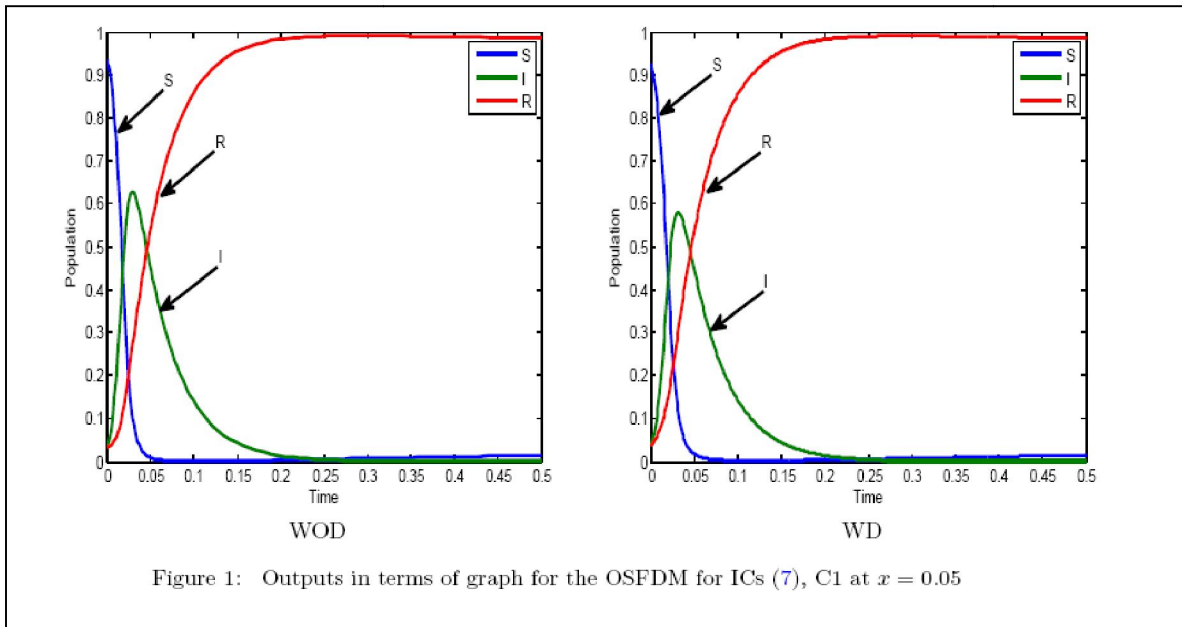
7. Numerical Solutions

Initial conditions given in Eq. (7) is being considered. The parameters values as mentioned in Table. 1 are used in numerical solution of the model given in Eqs. (1)-(3). The two points have been taken from the domain i.e. $x = 0.05$ and $x = 0.1$ and the analysis for all cases are conducted at these specific points for different days.

7.1 Initial condition (7) for case1 (C1) at $x = 0.05$

The outputs produced by OSFDM with the initial condition (7) for the C1 at $x = 0.05$ WD and WOD are illustrated in Fig. 1. The numerical outputs of the OSMM and the EMM regarding initial condition (7) are illustrated in Fig. 2. The number of susceptible quickly decreases while the number of infected quickly grows in the beginning due to interaction between susceptible and infected individuals and the number of recovered individuals quickly increases in the case of WOD model. The results produced by OSFDM,

OSMM and EMM are similar to the results of WOD model but the peak value of infected class in model WD is smaller than the peak value in WOD model. The susceptible class tends towards zero after $t = 0.05$ in the case of WOD model while in the model WD, the susceptible class tends towards zero after $t = 0.07$. This is due to mobility (diffusion). Also WD, the three classes get to steady state early as compared to WOD model.





8. Conclusions

In this paper we have added a uni-directional diffusion process to the SIR model. The models are simulated using finite difference and meshless procedures. Simple explicit and operator splitting schemes are used for time integrations. As a result of these numerical simulations, we compared performance of these schemes and the other hand we got insight into the effects of diffusion on this model.

References

- [1] C. D. Marchant S. F. Reising C. Christie, M. L. Marx, The 1993 epidemic of pertussis in Cincinnati resurgence of disease in a highly immunized population of children, *N. Engl. J. Med.* 331(1) (1994), no. 16-21.
- [2] S. Scott C. J. Duncan, S. R. Duncan, Whooping cough epidemic in London, 1701-1812: infection dynamics seasonal forcing and the effects of malnutrition, *Proc. R. Soc. Lond.* 263 (1996), no. 445-450.
- [3] N. H. carbonetti, "immunomodulation in the pathogenesis of bordetella pertussis infection and disease", *Curr. Opin. Pharm.* 7 (June 2007), no. 272-278.
- [4] J. D. Cherry, The epidemiology of pertussis and pertussis immunization in the United Kingdom and the United States: a comparative study, *Curr. Probl. Pediatr.* 14(2) (1984), no. 1-78.
- [5] N. Cox, The war on whooping cough: The impact of prevalence elasticity and state policies on vaccination behavior, *Depar. of Econ. Stan. Univ.* (May 2012), no. 1-59.
- [6] P. Van den Driesche and J. Watmough, Reproduction numbers and sub-threshold endemic equilibria for the compartmental models of disease transmission, *Math. Biosci.* 180 (2005), no. 29-48. 5
- [7] B. M. C. Charpentier G. G-Parra, A. J. Arenas, Combination of nonstandard schemes and Richardson's extrapolation to improve the numerical solution of population models, *Math. and Comp. Model.* 52 (2010), no. 1030-1036.
- [8] J. D. Nelson, The changing epidemiology of pertussis in young infants: the role of adults as reservoirs of infection, *Am. J. Dis. Child.* 132(4) (1978), no. 371-373.



Conference Proceedings SPI 2014 [18-22]

Cost Effective Approach for Risk Analysis of Natural Gas Pipelines

Muhammad Noman¹, Saeed Gul²

^{1,2} Department of Chemical Engineering, UET Peshawar. , Pakistan.

¹chemineer60@gmail.com, ²saeedgul@nwfpuet.edu.pk

Abstract:

Pipelines carrying natural gas are not on secure industrial site as a potentially hazardous plant, but are routed across the land, i.e., busy city or a network of superhighways. Consequently, there is the ever-present potential of incidents due to third party intervention, corrosion defects, construction defects and ground movement to interfere with the integrity of these pipelines. Pipeline accidents often result in consequences which have impacts of different dimensions. In this study, an approach will be developed to express the risk for a gas pipeline in terms of cost. Total cost consists of cost of repair, material loss and damage to humans and buildings. Data analysis of each incident category will be carried out by which the risk of city gas pipelines can be assessed. This study present data on loss of gas incidents to present a safety performance which helps natural gas company to analyze impacts of each incident category and optimize the resources and devise more effective preventive maintenance programs.

Keywords: risk; Incident; consequence; frequencv.

1. Introduction

As the cities expanded and people became aware of clean energy, the consumption of gas in cities increased dramatically from the 1980s in Pakistan. In order to meet the increased demand, the gas pipeline network carried larger quantities of gas at higher pressures, which implies that city gas facilities, including the gas pipelines, have to be operated more carefully than ever.

Natural gas is currently one of the most widely used sources of energy, and its use is growing. Nowadays, natural gas covers more than 50% [Pakistan Energy Breakup Statistics 2008-2009][17] of energy consumption in the Pakistan in different sectors like Domestic, Power, General Industry, Compressed Natural Gas(CNG). Pakistan has natural gas pipeline of hundreds of kilometers, which spreads all over the cities, distributed around and has various types of valve well, numerous grooves, underground structures and other confined spaces. Owing to the characteristics of flammability, high energy and pressure, noxiousness, harm, continuous operation, excessive points and large length, complex environment, once the gas pipelines are broken, it is very likely to cause fire, explosion and other serious accidents [13]. The safety problem of gas pipeline not only affects safe and normal pipeline transport and normal gas supply for enterprises and residents, but also threatens safety and living environment of people. In the recent years, more and more authorities have been aware of the safety problems of natural gas pipelines..



In 2004, fourteen people were killed and more than two hundred people were injured due to the explosion of a natural gas factory in Belgium. In Paraguay, a conflagration caused by gas leakage resulted in more than 250 deaths in 2004. In 2009, an explosion caused by gas leakage induced the greatest conflagration in Moscow ever since the Second World War. It is very important to analyze and assess effect of gas pipeline leakage and ruptures in terms of cost in cities and towns and take measures to improve its safety.

2. Risk Cost Relationship

Risk is defined as, “Combination of the likelihood of an occurrence of a hazardous event or exposure(s) and the severity of consequences caused by event or exposure(s)”.

$$\text{Risk} = \text{Consequence} \times \text{frequency}$$

In this study, an approach will be made to express the risk for a gas pipeline incident in terms of cost.[1]

$$\text{Total risk} = \text{Total cost}$$

$$\text{Risk} = \text{Consequence} \times \text{frequency}$$

$$\text{Cost} = \text{Risk}_{\text{Total}} = \sum C_s \times F_s$$

Risk will be found in terms of cost of each incident bear by company. Total cost consists of cost of repair, material loss and damage to humans and buildings.

$$C_{\text{total}} = C_{\text{material loss}} + C_{\text{human fatality/Injury}} + C_{\text{repair}}$$

In this research work criteria for incident is defined as, an event which lead to unintentional release of gas. In pipeline industry, Incident occurs due to many reasons but we will consider following six incident categories in our study. [3]

1. *Incident due to 3rd party excavation works.* For example digging, piling, ground works by following equipment anchor, bulldozer, excavator and plough can result in damage of pipeline.
2. *Incident due to Construction defect / material failure.* The type of defect (construction or material). The defect details (hard spot, lamination, material, field weld or unknown).
3. *Incident due to corrosion defects in pipeline.* For example external and internal corrosion can result in galvanic, pitting and stress corrosion cracking resulting in damage of pipeline.
4. *Incident due to ground movement* like dike break, erosion, flood, landslide, mining, river or unknown can result in damage of pipeline.
5. *Incident due to hot tape made by error.*
6. *Incident due to other and unknown.* (The sub-causes of category such as design error, lightening, maintenance).

3. Methodology

3.1 Frequency Evaluation

Frequency incidents will be found from incident statistics and Gas Leakage Detection (GLD) survey of Natural Gas Pipeline Company for certain geographic network in year 2011, 2012 and 2013

Events of unintentional release of gas are further categorized in following three sizes.



Table 1. Categories of leak sizes

Small scale leak (Pinhole/crack)	The diameter of the hole is smaller than or equal to 2cm.
Large scale release (Hole)	The diameter of the hole is larger than 2cm and smaller than or equal to the diameter of the pipe.
Rupture	The diameter of the hole is larger than the pipeline diameter.

Primary failure frequencies for each incident cause and ignition probability for each leak type is taken from ECIG Group report 2011 [3] and shown in table 2 and 3 respectively.

3.1 Consequence Evaluation

Consequences of incidents are gas release and fire eruption. These two causes will be analyzed in terms of small scale leak, large scale release and rupture of gas pipeline.

- For rupture incident in above cases, gas release will be found from incident statistics of Natural Gas Pipeline Company for year 2011, 2012 and 2013.
- For small scale leak and large scale release, gas release will be found from Gas Leakage Detection (GLD) survey for year 2011, 2012 and 2013.

Table 2: Distribution of incident per cause

Cause	Distribution [%]
External Interferences	48.4
Construction defects	16.7
Corrosion defects	16.1
Ground Movement	7.4
Hot tape made by Error	4.8
Others and unknown	6.6

Table 3: Ignition Probabilities

Size of leak	Ignition Probabilities [%]
Small scale leak	4
Large scale release	2
Rupture	13

The cost of lost gas depends on response time. Response time refers to time to recognize accidental release, to move to release point and to shut down the block valve or repair the release point instantly. The response time of small-scale leak is assumed to be three (03) days and that of large-scale release is assumed to be one (01) day. In case of rupture of pipeline instant action will be taken to shut down the supply.

Eruption of fire will result in fatality / burn injury of human being and damage to building. The cost of human damage was estimated in terms of heavy, medium and light injury is assumed to be 50, 10 and 1% of the cost of fatality. The cost of building damage is estimated by the summation of construction and interior repair costs.

4. Results and Discussions

Here we will consider three (03) years data of Natural Gas Pipeline operator for a certain geographic network. Cost of natural gas considered here is Rs 300 / MMCF. Total loss of gas due to small scale leak, large scale release and rupture for each year is presented below after calculation.

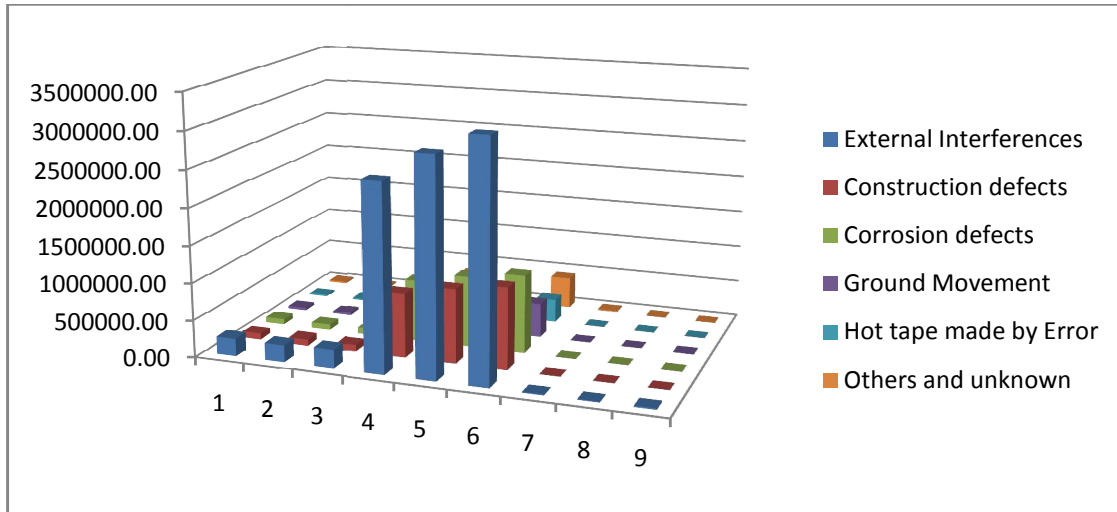


Figure 1: Cost comparison regarding each incident cause.

It has been evident from Figure 1 that external interferences are biggest threat to pipeline safety, causing a major gas release followed by construction defects and corrosion defects

4. Preventive Maintenance Program

As evident from above figures external interference, corrosion defects and construction defects are the largest cause of accidents to pipelines. In order to develop cost effective approach for risk reduction, preventive maintenance program is put down in order to address major threats to natural gas pipeline safety.

One call Notification System: One-call notification centers functions as a communication system established by a gas pipeline company, government agencies, or other operators of underground facilities to provide one telephone number for notification of excavating, tunneling, demolition, or any other similar work. [6]

Gas safety management system: Prior to performing any excavation job, meeting shall be carried out for finalizing the nature of activity, time schedule and for exchanging as-built drawings of the network where the activity is going to be carried out. In order to ensure proper communication between pipeline operator and 3rd parties “Gas Safety Management Activity Performa” is developed which should be filled before execution of job.

Pre-marking and Underground Detection Technologies: Pre-marking an intended excavation site to specifically indicate the area where underground facilities need to be identified is a practice that helps prevent excavation damage. It is also recommended to determine the exact location “by safe and acceptable means” to approach the estimated location during excavation.

Employees qualifications and trainings: Training to prevent excavation damage to the underground infrastructure is not limited to the pipeline industry and operating personnel: locators need training in locating techniques, equipment technology, and marking procedures; excavators need training to fully participate in the notification process and to understand locator marking symbols; one-call operators need training to efficiently and effectively transmit information between excavators and underground system operators; and the general public needs to be aware of the one-call notification process when they dig for private projects.

Emergency Response Plan: Pipeline operators are required by law to establish written emergency procedures for classifying events that require immediate response, communicating with emergency response officials, and responding to each type of emergency, emergency response planning should involve a definition of responsibilities,



a flow chart of actions, execution criteria, systems inventory and resource information, coordination procedures (internal and external), and simulation exercises of response actions.

Sabotage: In order to counter any sabotage activity, gas pipeline operator is responsible for the patrolling at right of way (ROW) and also shall develop liaison on special request basis with the security agencies in this regard. Proper maintenance of acquires / purchased ROW without any encroachment.

Quality Assurance system for construction defects should be in place during construction phase of pipeline in order to avoid failure of pipeline. *Effective Corrosion Protection (CP) system* should be in place in order to protect pipeline form corrosion damages. GLD survey will be utilized for identification of small scale leak and large scale release from pipeline. *Reduction in response time* for risk reduction in terms of cost

4. Conclusion

Urbanization of lands through which gas pipelines are routed, combined with an increase in the number of users of the underground, has created complications for the natural gas pipeline operators. In this study an approach has been made to analyze the incident cost incurred to natural gas operator due to accidental release from pipeline. Each cost category is analyzed and their impact is discussed. The high contribution of external interference followed by corrosion defects and construction defects emphasizes its importance to pipeline operators and authorities. Preventive maintenance program is put down in order to address major threats to natural gas pipeline safety in order to satisfy the criteria of the gas company.

References

- [1] Park, K. -S., Lee, J. -H., and Jo, Y. -D. (2004). An approach to risk management of city gas pipeline. *Process Safety and Environmental Protection*, 82(B6), 446-452.
- [2] Stephens, M. J. (2000). A model for sizing high consequence areas associated with natural gas pipelines, GRI Report no: GRI-00/ 0189.
- [3] 8th report of the European gas pipeline incident data group. (2011). EGIG 11.R.0402 (version 2).
- [4] Jo Y. -D, and Ahn. B. J. (2003). A simple model for the release rate of hazardous gas from a hole on high pressure pipelines, *Journal of Hazardous Materials*, 97(1-3): 31-46.
- [5] Mannan, S. (2005). *Lees' loss prevention in the process industries*. 3rd Edition, Elsevier Butterworth -Heinemann, USA.
- [6] Protecting public safety through excavation damage preventions. (1997). *Safety Study*, National Transportation Safety Board, Washington D.C.
- [7] Burgherr, P., and Hirschberg, S. (2005). *Comparative assessment of natural gas accident risks*, Paul Scherrer Institute, Switzerland.
- [8] Jo Y. -D., and Crowl D. A. (2008). Individual risk analysis of high-pressure natural gas pipelines. *Journal of Loss Prevention in Process Industries*, 2, 589-595.
- [9] Jo Y. -D, and Ahn. B. J. (2005). A method of quantitative risk assessment for transmission pipeline carrying natural gas. *Journal of Hazardous Material*, A123, 1-12.
- [10] Han. Z. Y., and Weng W. G. (2010). An integrated quantitative risk analysis method for natural gas pipeline network. *Journal of Loss Prevention in the Process Industries*, 23, 428-436.
- [11] Han. Z. Y., and Weng W. G. (2011). Comparison study on qualitative and quantitative risk assessment methods for urban natural gas pipeline network. *Journal of Hazardous Material*, 189, 509-518.
- [12] Slavounos, S., and Rigas, F. (2006). Estimation of safety distances in the vicinity of fuel gas pipelines. *Journal of Loss Prevention in the Process Industries*, 19, 24-31.
- [13] Zhenghua, H., and Jianhua, L. (2012). Assessment of fire risk of gas pipeline leakage in cities and town. *Procedia Engineering*, 45, 77-82.
- [14] Risk based inspection base resource document. (2002). First edition. API recommended practice 580.
- [15] Pakistan Energy Breakup - Statistics 2008-2009



Conference Proceedings SPI 2014 [23-27]

Numerical simulation of pure diffusion model by Haar wavelets Muhammad Ahsan¹, Siraj-Ul-Islam²

^{1,2} Department of Basic Sciences, NWFP University of Engineering and Technology,
Peshawar, Khyber Pakhtunkhwa, Pakistan

¹ahsan_kog@yahoo.com, ²siraj.islam@gmail.com

Abstract:

In this paper we present a new collocation method based on Haar Wavelets for the numerical solution of the Pure Diffusion Model (PDM). This method is the extension of the Haar wavelet method [4] with same accuracy. In the present method the time discretization is performed by forward difference operator and the spacial derivatives are approximated by Haar Wavelets. The advantage of the present method to Haar Wavelet method [4] is the time efficiency. As well as this method can also be applied to Partial Differential Equations (PDE) with Neumann and Robin boundary conditions easily as compared to Finite Difference Method (FDM). The numerical results of simple diffusion equation with Dirichlet jump boundary conditions also favorably match with the exact solutions.

Keywords: Haar wavelets, Pure Diffusion Model (PDM), Dirichlet boundary condition, Collocation method.

1. Introduction

In this paper, we propose a new collocation method based on Haar Wavelets for the numerical solution of the following 2-Dimensional Pure Diffusion Model (PDM),

$$\frac{\partial u(x,y,t)}{\partial t} = K \left(\frac{\partial^2 u(x,y,t)}{\partial x^2} + \frac{\partial^2 u(x,y,t)}{\partial y^2} \right), \quad 0 < x,y < 1, \quad t > 0; \quad (1)$$

with Dirichlet time- dependent boundary conditions,

$$u(0,y,t) = f_1(y,t), \quad u(1,y,t) = f_2(y,t), \quad 0 \leq y \leq 1, \quad 0 \leq t \leq T,$$

$$u(x,0,t) = g_1(x,t), \quad u(x,1,t) = g_2(x,t), \quad 0 \leq x \leq 1, \quad 0 \leq t \leq T,$$

with initial condition given as,

$$u(x,y,0) = f(x,y), \quad 0 < x,y < 1,$$

where K is any function of x and y or constant.



The PDM have many applications in physics, mechanics and engineering. Many methods have been used for the numerical solution of PDM. Recent contributions for numerical solution are Wavelets Method (WM) [4] and Meshless Methods (MM) based on Multiquadric Radial Basis Functions (MQRBFs) [5] and other methods like Finite Difference Method (FDM) [1] and Finite Element Method (FEM) [2, 3] have also been used for the numerical solutions of Partial Diffusion Equations in the literature.

1.1 Haar wavelets

The Haar wavelet family for $x \in [0, 1]$ is defined as

$$h_i(x) = \begin{cases} 1 & \text{for } x \in [\alpha, \beta), \\ -1 & \text{for } x \in [\beta, \gamma), \\ 0 & \text{elsewhere,} \end{cases} \quad (2)$$

Where $\alpha = \frac{k}{m}$, $\beta = \frac{k+0.5}{m}$ and $\gamma = \frac{k+1}{m}$.

In the above definition integer $m = 2^j$; $j = 0, 1, \dots, J$, indicates the level of the wavelet and integer $k = 0, 1, \dots, m-1$ is the translation parameter. Maximum level of resolution is J . The index i in Eq. (2) is calculated using the formula $i = m + k + 1$. In case of minimal values $m = 1$; $k = 0$, we have $i = 2$. The maximal value of i is $i = 2M = 2^{J+1}$. For $i = 1$, the function $h_1(x)$ is the scaling function for the family of Haar wavelets which is defined as

$$h_1(x) = \begin{cases} 1 & \text{for } x \in [0,1), \\ 0 & \text{elsewhere.} \end{cases}$$

We define the following notations

$$p_{i,1} = \int_0^x h_i(x) dx$$

and

$$p_{i,2} = \int_0^x p_{i,1}(x) dx$$

So using Eq.(2) we get

$$p_{i,1}(x) = \begin{cases} x - \alpha & \text{for } x \in [\alpha, \beta), \\ \gamma - x & \text{for } x \in [\beta, \gamma), \\ 0 & \text{elsewhere,} \end{cases}$$

and

$$p_{i,2}(x) = \begin{cases} \frac{(x-\alpha)^2}{2} & \text{for } x \in [\alpha, \beta), \\ \frac{1}{4m^2} - \frac{(\gamma-x)^2}{2} & \text{for } x \in [\beta, \gamma), \\ \frac{1}{4m^2} & \text{for } x \in [\gamma, 1) \\ 0 & \text{elsewhere.} \end{cases}$$



2. Solution procedure for space derivatives by Haar wavelets

Consider the given Haar wavelet approximation:

$$\frac{\partial^4 u}{\partial x^2 \partial y^2} = \sum_{i=1}^{2M} \sum_{j=1}^{2M} b_{ij} h_i(x) h_j(y) \quad (3)$$

Partially integrating Eq. (3) w.r.t x, from 0 to x, we get

$$\frac{\partial^3 u}{\partial x \partial y^2} = \sum_{j=1}^{2M} \alpha_j h_j(y) + \sum_{i=1}^{2M} \sum_{j=1}^{2M} b_{ij} P_{i,1}(x) h_j(y) \quad (4)$$

$$\text{Where } \frac{\partial^3 u(0,y)}{\partial x \partial y^2} = \sum_{j=1}^{2M} \alpha_j h_j(y)$$

Again partially integrating Eq. (4) w.r.t x using the limits 0 to x, we have

$$\frac{\partial^2 u}{\partial y^2} = \sum_{j=1}^{2M} \beta_j h_j(y) + x \sum_{j=1}^{2M} \alpha_j h_j(y) + \sum_{i=1}^{2M} \sum_{j=1}^{2M} b_{ij} P_{i,2}(x) h_j(y) \quad (5)$$

In the same way, two times integrating Eq.(3) w.r.t y with limits 0 to y, we get the following expression

$$\frac{\partial^2 u}{\partial x^2} = \sum_{i=1}^{2M} \sigma_i h_i(x) + y \sum_{i=1}^{2M} \delta_i h_i(x) + \sum_{i=1}^{2M} \sum_{j=1}^{2M} b_{ij} P_{j,2}(y) h_i(x) \quad (6)$$

Integrating Eq.(5) from 0 to y w.r.t. y we get

$$\frac{\partial u}{\partial y} = \frac{\partial u(x,0,t)}{\partial y} + \sum_{j=1}^{2M} \beta_j P_{j,1}(y) + x \sum_{j=1}^{2M} \alpha_j P_{j,1}(y) + \sum_{i=1}^{2M} \sum_{j=1}^{2M} b_{ij} P_{i,2}(x) P_{j,1}(y) \quad (7)$$

As $\frac{\partial u(x,0,t)}{\partial y}$ is unknown so again integrating Eq.(7) from 0 to 1 w.r.t. y we get

$$U(x,1,t) - u(x,0,t) = \frac{\partial u(x,0,t)}{\partial y} + \sum_{j=1}^{2M} \beta_j P_{j,2}(1) + x \sum_{j=1}^{2M} \alpha_j P_{j,2}(1) + \sum_{i=1}^{2M} \sum_{j=1}^{2M} b_{ij} P_{i,2}(x) P_{j,2}(1) \quad (8)$$

Eliminating $\frac{\partial u(x,0,t)}{\partial y}$ from Eq.(7) and Eq.(8) and using the boundary conditions, we obtain the following expressions.

$$\frac{\partial u}{\partial y} = \sum_{j=1}^{2M} \beta_j (P_{j,1}(y) - P_{j,2}(1)) + x \sum_{j=1}^{2M} \alpha_j (P_{j,1}(y) - P_{j,2}(1)) + \sum_{i=1}^{2M} \sum_{j=1}^{2M} b_{ij} P_{i,2}(x) (P_{j,1}(y) - P_{j,2}(1)) \quad (9)$$

integration Eq.(9) and further simplification we get

$$u(x,y,t) = \sum_{j=1}^{2M} \beta_j (P_{j,2}(y) - P_{j,2}(1)) + x \sum_{j=1}^{2M} \alpha_j (P_{j,2}(y) - y P_{j,2}(1)) + \sum_{i=1}^{2M} \sum_{j=1}^{2M} b_{ij} P_{i,2}(x) (P_{j,2}(y) - y P_{j,2}(1)) \quad (10)$$

Similarly two times integrating Eq.(6) from 0 to x w.r.t x we get

$$u(x,y,t) = \sum_{j=1}^{2M} \delta_j (P_{i,2}(x) - x P_{i,2}(1)) + y \sum_{j=1}^{2M} \gamma_j (P_{i,2}(x) - x P_{i,2}(1)) + \sum_{i=1}^{2M} \sum_{j=1}^{2M} b_{ij} P_{j,2}(y) (P_{i,2}(x) - x P_{i,2}(1)) \quad (11)$$

Comparing Eq. (11) and (12) and putting $x = 0; 1$, $y = 0; 1$ respectively we get $8M$ equations in $4M^2 + 8M$ unknowns. Time discretizing Eq.(1) we get

$$u(x, y, t) = u(x, y, t_0) + \Delta t K \left(\frac{\partial^2 u(x, y, t)}{\partial x^2} + \frac{\partial^2 u(x, y, t)}{\partial y^2} \right) \tag{12}$$

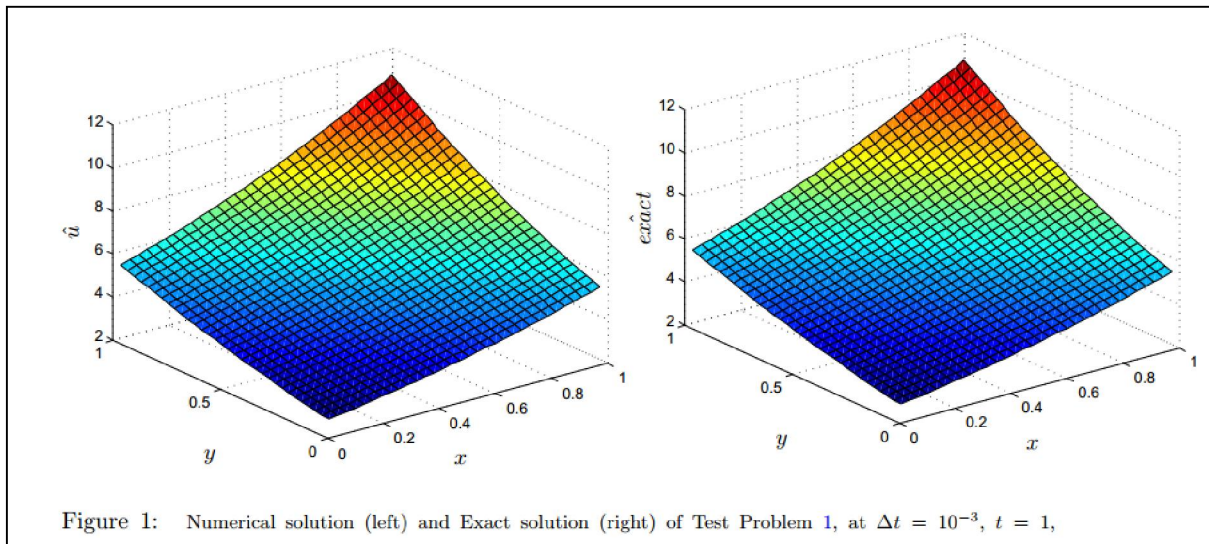
Where $u(x, y, t_0)$ is the previous time level solution. By putting any one expressions of u and its partial derivatives into Eq.(12) we get another system of $4M^2$ equations with $4M^2 + 8M$ unknowns. Now we have $4M^2 + 8M$ equations in $4M^2 + 8M$ unknowns. These system of equations are solved simultaneously for the Haar coefficients. The solution can be find by putting these Haar coefficients in any expression of $u(x, y, t)$.

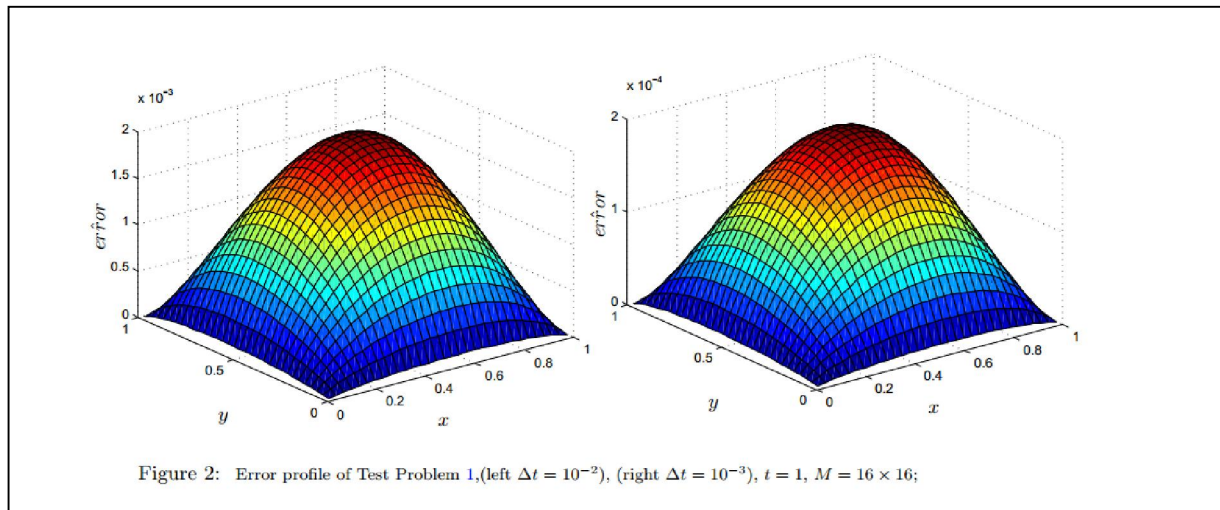
3. Results and Discussions

Test Problem 1. In the Eq. (1) $K=1$, the exact solution is given by

$$u(x, y, t) = e^{\frac{x+y}{\sqrt{2}}+t}$$

The initial and boundary conditions are obtained from the exact solution. In Table 1 the maximum absolute errors for different number of collocation points are given with CPU time of present method. In figure 1 the numerical and exact solution profiles are given to checked the accuracy of the proposed method. The resemblance between numerical and exact solutions is clear from these figures. The numerical results in terms of absolute error of the proposed methods for different time steps are shown in figure 2.





References

- [1] A.R. Abdullah D.J. Evans. New explicit method for the solution of $\frac{\partial u}{\partial t} = \frac{\partial^2 u}{\partial x^2} + \frac{\partial^2 u}{\partial y^2}$. Int. J. Comput. Math., 14:325-353, 1983.
- [2] C.A.J. Fletcher. A comparison of finite element and finite difference solution of the one and two dimensional burgers equations. Comput. Phys., 51:159-188, 1983.
- [3] Liu GR. Mesh free methods: moving beyond the finite element method. Boca Raton: CRC Press; 2003.
- [4] Siraj ul Islam, Imran Aziz, A.S. Al-Fhaid, and Ajmal Shah. A numerical assessment of parabolic partial differential equations using haar and legendre wavelets. Appl. Math. Modelling, 37:9455-9481, 2013.
- [5] G. Yao, Siraj ul Islam and Bozidar Sarle. A comparative study of global and local meshless method for diffusion-reaction. CME, 59:127-154, 2010.



Conference Proceedings SPI 2014 [28-33]

Numerical Solution Method of Highly Oscillatory 1D Fredholm Integral Equation

Tariq Mahmood¹, Siraj-ul-Islam²

^{1,2} Department of Basic Sciences, University of Engineering & Technology, Peshawar, Pakistan, PO Box 814, Post code 25120

¹tmkhan036@hotmail.com, ²siraj.islam@gmail.com

Abstract:

A new numerical method is put forward for the solution of highly oscillatory Fredholm integral equations of the second kind using Multi Quadric Radial Basis Functions (MQRBF). The method is based on the Levin's principal of converting the integration problem into a differential equation. The differential equation is then solved by a meshless method. Numerical examples show the accuracy of the proposed method for high frequency ω .

Keywords: Fredholm integral equations, MQRBF, Levin Method

1. Introduction

The Fredholm integral equations (FIEs) have gained popularity in the field of Engineering and Science, covering a long range of applications. The FIE of the second kind can be expressed as [1, 2]:

$$\psi(x) = h(x) + \int_a^b K(x, y) \psi(y) dy, \quad (1)$$

Where $a, b \in \mathbb{R}$ and ψ is an unknown function needs to be approximated. $K(x, y)$ is a highly oscillatory kernel function. The literature is not providing sufficient information in this regard. For non oscillatory kernels the authors [3, 4, 5, 6] have presented numerical methods for FIEs. The solution of such IE's relies on the solution of the highly oscillatory integral involved in the IE's. For IE's having HOKs of the type $(f(x, y)e^{i\omega g(x, y)}, \omega \gg 1)$, traditional methods like Simpson's and Gauss Quadrature rules fail to provide an accurate approximation of the IE's especially when the number of quadrature points is less than the frequency ω . In [7], the authors have presented an efficient MQRBF approximation for the integrals with highly oscillatory kernels. The method is accurate as well as efficient to approximate the integral for larger frequency. The work in the present paper is the extension of our earlier work [7] from HOIs to highly oscillatory integral equations.

1.1 RBF Based Differential Quadrature Method

A univariate function $\phi(r)$, where $r \geq 0$ is a RBF together with the Euclidean norm. For the given N centers $x_1^c, x_2^c, x_3^c, \dots, x_N^c$, the RBF interpolant has the form

$$s(x) = \sum_{j=1}^N \alpha_j \phi(\|x - x_j^c\|_2, \varepsilon), \quad (2)$$



where ε is a free shape parameter. The co-efficient α_j can be determined by the interpolation condition

$$s(x_j) = f_j, \quad (3)$$

at the set of points located at N centers. Enforcing the interpolation condition, we obtain a system of linear equations

$$\mathbf{B}\alpha_j = f_j, \quad (4)$$

which can be solved for the expansion co-efficient α_j . The interpolation matrix \mathbf{B} has the elements of the form

$$b_{mn} = \phi(\|x_m^c - x_n^c\|_2). \quad (5)$$

From Eq. (2) the m^{th} order derivative can be written as

$$s^m(x) = \sum_{j=1}^N \alpha_j \phi^m(\|x - x_j^c\|_2, \varepsilon). \quad (6)$$

2. Solution Procedure for FIE

The solution of FIE of the type (1) relies on the solution of the highly oscillatory integral

$$I_j = \int_a^b f(x_j, y) e^{i\omega g(x_j, y)} \psi(y) dy, \quad j = 1, 2, 3, \dots, N + 1. \quad (7)$$

As described in [8], we consider a function $p(y)$ satisfying the differential equation

$$f(x_j, y)\psi(y) = p'(y) + i\omega g'(x_j, y)p(y), \quad (8)$$

where the function $p(y)$ and its derivative are defined as

$$\left. \begin{aligned} p(y) &= \sum_{j=1}^{N+1} \alpha_j \phi_j \\ p'(y) &= \sum_{j=1}^{N+1} \alpha_j \phi_j' \end{aligned} \right\} \quad (9)$$

where $\phi_j = \sqrt{(y - y_j^c)^2 + \varepsilon^2}$. Subsequently, as a result (8) can be written as

$$f(x_j, y)\psi(y) = \sum_{j=1}^{N+1} \alpha_j \phi_j' + i\omega g'(x_j, y) \sum_{j=1}^{N+1} \alpha_j \phi_j. \quad (10)$$

In matrix notation form the above equation can be written as

$$\mathbf{B}\alpha = \mathbf{F}_j \circ \Psi, \quad (11)$$



where $\Psi = [\psi(y_1), \psi(y_2), \dots, \psi(y_{N+1})]^T$, $F_j = [f(x_j, y_1), f(x_j, y_2), \dots, f(x_j, y_{N+1})]^T$,

$\alpha = [\alpha_1, \alpha_2, \alpha_3, \dots, \alpha_{N+1}]^T$, and \circ denotes the Hadamard product.

$F_j \circ \Psi = \text{diag}(F_j)\Psi$ is a vector having entries $f(x_j, y_k)\psi(y_k)$, $k = 1, 2, 3, \dots, N + 1$.

Using (11) we have

$$\alpha = \mathbf{B}^{-1} \text{diag}(F_j)\Psi. \quad (12)$$

The value of α are used to get the following system of linear equations

$$\mathbf{P}_j = \sum_{j=1}^{N+1} \mathbf{B}^{-1} \text{diag}(F_j)\Psi \phi_j, \quad (13)$$

where $\mathbf{P}_j = [p(y_1), p(y_2), p(y_3), \dots, p(y_{N+1})]^T$. The first and last values of \mathbf{P}_j will be considered as $p(a)$ and $p(b)$ respectively. Subsequently (2) will be written as

$$I_j = \left(\left[-e^{\omega g(x_j, a)}, \dots, \dots, e^{\omega g(x_j, b)} \right] \right) \times \mathbf{B}^{-1} \text{diag}(F_j)\Psi \phi_j. \quad (14)$$

Let

$$\mathbf{S}_j = \left(\left[-e^{\omega g(x_j, a)}, \dots, \dots, e^{\omega g(x_j, b)} \right] \right) \times \mathbf{B}^{-1} \text{diag}(F_j)\phi_j. \quad (15)$$

So (14) becomes

$$I_j = \mathbf{S}_j \Psi, \quad (16)$$

where Ψ is still unknown.

Thus from (1) we have

$$\psi(x_j) = h(x_j) + \mathbf{S}_j \Psi. \quad (17)$$

In the above equation the unknown Ψ is based on the nodes in the “y” direction. So if $x = y$, the step size along x and y are same. Then

$$\psi(x_j) = \Psi = \psi(y_k) \quad (18)$$

Thus from Eq.(17) we have



$$\Psi = \mathbf{H} + \mathbf{S}\Psi$$

(19)

Where

$$\mathbf{S} = \begin{bmatrix} s_1 \\ s_2 \\ \vdots \\ s_{N+1} \end{bmatrix} \in \mathbb{C}^{(N+1) \times (N+1)}, \mathbf{H} = \begin{bmatrix} h(x_1) \\ h(x_2) \\ \vdots \\ h(x_{N+1}) \end{bmatrix} \in \mathbb{C}^{(N+1) \times 1}$$

From (19) the solution Ψ can be obtained as

$$\Psi = (\mathbf{I} - \mathbf{S})^{-1}\mathbf{H} \quad (20)$$

where \mathbf{I} is the identity matrix having the same dimension as \mathbf{S} .

3. Results and Discussions

In this section we are considering some test problems having an oscillatory character.

It should be noted that the value for the shape parameter “ ϵ ” is considered 0.5 throughout the examples. The table contains Maximum absolute and Relative Errors for comparative study. All the computations are carried out using *Dell Core i3* using *MATLAB R2009b* platform. The errors are defined below for comparative study.

$$\text{Absolute Error: } L_{ab} = \text{abs}(\text{approximate} - \text{exact})$$

$$\text{Relative Error: } L_{re} = \frac{\text{abs}(\text{approximate} - \text{exact})}{\text{abs}(\text{exact})}$$

3.1 Test Problem

Consider the following example in the interval [0,1]

$$\psi(x) = h(x) + \int_0^1 f(x,y)e^{t\omega g(x,y)} \psi(y) dy, \text{ with}$$

$$g(x,y) = \frac{x^2}{20} + \left(x + \frac{6}{5}\right)^2, \quad h(x) = \cos(10x) + \left(e^{\frac{1}{20}t\omega x^2 + \frac{36}{25}t\omega} - e^{\frac{1}{20}t\omega x^2 + \frac{121}{25}t\omega}\right)e^{-x^2}, \quad f(x,y) = \frac{t\omega(2y + \frac{12}{5})}{\cos(10y)} e^{-x^2}. \quad \text{The exact solution is } \psi(x) = \cos(10x).$$

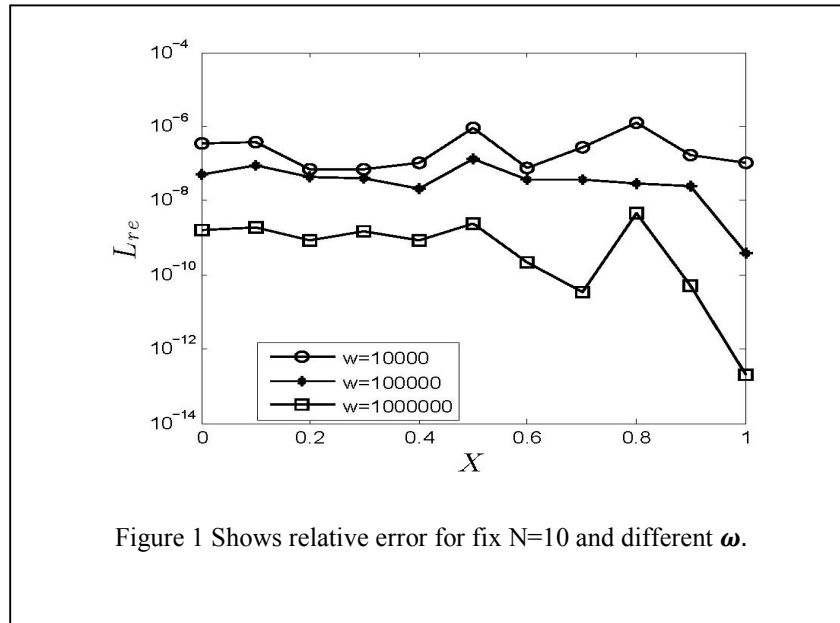


Table 1 Shows CPU time for different ω and fix N=10.

ω	10000	100000	1000000
L_{∞}	3.3781e-007	5.2204e-008	1.5660e-009

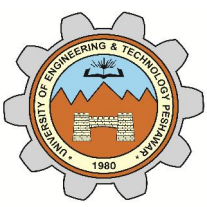
Table 3: Shows maximum absolute error for different ω and fix N=10.

ω	10000	100000	1000000
CPU time	0.045000	0.015116	0.038249

From the above two examples it is clear that we do not need any special nodes for the solution of highly oscillatory Fredholm integral equation of the second kind. Also we see that the method is stable and accurate as the frequency increases while low no of points are required to get the desire accuracy.

References

- [1] K. Atkinson. The Numerical solution of integral Equations of the Second Kind. Cambridge University Press, Cambridge, 1997.
- [2] L.Furong and W.Jing. An interpolation-based adaptive solution method for fredholm mintegral equations of the second kind. Journal of Natural Science of HeiLongJiang University, 21(4):17-21, 2004.
- [3] I.P. DOBROBOL'SKII. Richardson extrapolation in the approximate solution of fredholm integral equations of the second kind. U.S.S.R Comput. Maths. Maths. Phys, 21(4):139-149, 1981.



- [4] Z. Mahmoodi J. Rashidinia, E.Babolian. Spline collocation for fredholm integral equations. *Mathematical Sciences*, 5(2):147-158, 2011.
- [5] Guangqing Long and Gnaneshwar Nelakanti. Iteration methods for fredholm integral equation of the second kind. *comp and Mathematics with application*, (53):886-894, 2007.
- [6] Lothar Reichel. Fast solution methods for fredholm integral equations of the second kind. *Numerische Mathematik*, (57):719{736, 1990.
- [7] Sakhi Zaman Siraj-ul Islam, A.S. Al-Fhaid. Meshless and wavelets based complex quadrature of highly oscillatory integrals and the integrals with stationary points. *Engineering Analysis with Boundary Elements*, 37:1136{1144, 2013.
- [8] David Levin. Procedures for computing one- and two-dimensional integrals of fuctions with rapid irregular oscillations. *Mathematics for Computation*, 38(158):531 {538, 1982.



Conference Proceedings SPI 2014 [34-38]

Effect of CO₂ On The Growth Rate of Microalgae in a Photo Bioreactor (Pbr)

Asmatullah¹, Mohammad Younas²

*^{1,2}Department of Chemical Engineering, University of Engineering & Technology,
Peshawar, Pakistan, PO Box 814, Post code 25120*

¹engr.asmatullah@gmail.com, ²engr_unas@nwfpuet.edu.pk

Abstract:

For the past few years algae haven studied considerable as a research tool because of their nutritional value and their effective use in environment cleaning. Nowadays, algae are also considered as an alternate source of energy. High growth rates of algae are the focus of researchers in current era which lies in the efficient design of photo bioreactors. However CO₂ is also an important restrictive factor in micro-algae growth. The advantage of use of CO₂ in the growth of microalgae is that it can counteract the adverse effects of CO₂ production by industrial activities on environment. CO₂ is the major specie of greenhouse gases which caused global debates concerning climate alteration. One of the options to mitigate the adverse effects of CO₂ emission is to utilize CO₂ aquatic microalgae growth. Other advantage of use of CO₂ in the production of microalgae is to convert the CO₂ into algal biomass, which can in turn used in many applications, such as biofuels, organic fertilizers, stock feeds and pharmaceuticals products.

The aim of current study is to determine the optimum concentration of CO₂ for high growth rate of microalgae biomass. In this research a photo bioreactor (PBR) was fabricated and installed for microalgae cultivation. Air and CO₂ mixed was injected into Photo bioreactor (PBR) under various concentrations (0%, 10%, 20%, 30% (v/v in air)) while keeping other factors such as temperature, light intensity, PH and growing medium composition constant. Results showed that the growth of microalgae increased significantly by increasing CO₂ concentration. Growth rate (cells/ml) of microalgae was analyzed verses different CO₂ concentrations. The operating conditions will be considered for the developing of operational strategies and in projects of photo bioreactors for carbon-dioxide mitigation through microalgae.

Keywords: *Microalgae, CO₂ mitigation, biofuels, photobioreactor.*

1. Introduction

Carbon dioxide mitigation is the effort to prevent or reduce the emission of CO₂ gas into atmosphere. This includes the use of modern technologies, renewable energies, modification in older equipment to make them energy efficient and change of customer's behavior. To meet the need for energy in this industrial age, the rapid use of fossil fuel such as oil, gas and coal has caused a remarkable increase in carbon dioxide (CO₂) concentration in the atmosphere. The concentration of CO₂ in flue gas is 10 to 20% depending upon the burning fuel source [1]. This increase in the concentration of CO₂ in the atmosphere is causing measurable increase in global warming [2]. The potential adverse



effects of global warming include sea-level rise, floods, increased intensity of wildfires, draughts and storms. It also brings changes in the amount, distribution and timing of rain and snow. High level of CO₂ in atmosphere also increases the absorption of CO₂ by sea water which causes the ocean more acidic with potentially adverse effects on marine planktons. Economically feasible methods are needed to mitigate the effect of increased CO₂ level. The use of microalgae is a best option for biological CO₂ mitigation.

Microalgae are the simplest plants that contain chlorophyll and are able to produce organic compounds by absorbing water and CO₂ in the presence of sunlight through the process of photosynthesis. The biomass micro-algal molecular formula suggests that H₂O, CO₂, sunlight and other nutrients are the nutritional requirements for the growth of microalgae [3]. The following reaction shows the process of photosynthesis in microalgae.



An attempt to reduce the concentration of carbon-dioxide (CO₂) in the atmosphere, a biological approach of cultivating microalgae is used. The biomass is processed to make valuable products such as biofuels, pharmaceutical products, fertilizers and stock feeds [4]. Other factor such as temperature, light intensity and mixing rate also affects micro-algal growth. There is no single answer to the question, which of the various methods and technologies of microalgae harvesting should be used for optimum product achievement. Algae size plays an important role in choosing the suitable option. Low cost filtration techniques are presently used only for large size microalgae. On the other hand flocculation is used for small size microalgae. Cell mobility also affects the flocculation process. Sedimentation and flotation is also used depending upon the density difference between Microalgal cell and the growth medium. Moreover, oxygen released during photosynthesis support the use of flotation method. A basic criterion for selecting the harvesting method is the final algae paste concentration [5].

The increase in global warming, which is due to the elevated carbon-dioxide (CO₂) concentration in the atmosphere, is a challenge for the scientists in this industrial era. To reduce the emission of greenhouse gases (GHG) by 5.2%, the United Nations has signed an agreement (Kyoto protocol, 1997). This protocol has been signed by more than 170 countries of the world [6]. Different CO₂ mitigation methods have been applied, which can be classified into two categories. (i) Chemical reaction based CO₂ mitigation (ii) biological CO₂ mitigation. The chemical reaction based method is further divided into three procedures (a) separation (b) transportation (c) sequestration of CO₂. The chemical reaction based approach is relatively costly. For transportation purposes the cost of CO₂ separation and compression to 110 bars is more than \$30 per ton of CO₂, also the cost of CO₂ transportation is estimated to be \$1 to 3 per ton per 100km and sequestration cost is \$1 to 3 per ton of CO₂ [7]. As the above mentioned methods are more energy consuming and relatively costly, therefore it is necessary to develop such methods which are cost effective and suitable alternatives.

Many attempts have been made to reduce the quantity of CO₂ in the atmosphere. The use of biotechnology has extensively been studied since the beginning of the 1990's. The best option is biological CO₂ mitigation. This method is more attractive because the algal biomass formed as byproduct during the CO₂ fixation through the process of photosynthesis used for the production of biofuel. Microalgae can mitigate the adverse effect of CO₂ and produce bioenergy, and is a good candidate to replace second generation biofuels with third generation biofuels [8].

2. Material and Methods

Water samples were collected from various lakes of KPK using 0.45 micron plankton net. The micro-algal strains were enriched on a medium called Chu 13 modified medium which contained 0.2 g/L KNO₃, 0.1 g/L MgSO₄, 0.04 g/L K₂HPO₄, 0.054g/L CaCl₂.2H₂O, 0.1g/L citric acid, 0.01g/L ferric citrate, and 1mL of microelement solution containing different compounds, i.e. 2.85 g/L H₃BO₃, 0.02 g/L ZnSO₄.7H₂O, 1.80 g/L MnCl₂, 0.08 g/L CuSO₄.5H₂O, 0.05 g/L MoO₄.2H₂O and 0.08 g/L CoCl₂.6H₂O. The pH recorded for this medium was 6.6. The culture containing the medium was transferred to photobioreactor. The temperature was kept between 25-27 °C, with 24h lighting. The photobioreactor were consists of 4 transparent plastic bottles each having one liter volume. For a carbon source CO₂ gas was employed through a cylinder. A prescribed ratio of CO₂ mixed with air was supplied to the culture through air diffuser. Three 25 watt, Philips were used as a source of light. Different CO₂ concentrations (0, 10, 20 and 30%) were obtained by mixing ambient air with pure CO₂ and the mixture was aerated into the

photobioreactor. Cell counting was done using a hemocytometer. The flow rate was kept at 20ml/min using a volume flow meter. The culture was examined on daily basis for pH and cell density. Each experiment was performed in triplicate for the same conditions.

3. Results and Discussion

The present study shows that increasing the concentration of carbon dioxide led to an increase in cell growth rate of microalgae. The effect of increasing CO₂ injecting on culture growth rate (cell/mL) was in agreement with the Molina (2000) research report which shows that the more CO₂ concentration, the higher will be the growth rate of microalgae. Qui and Gao [9] showed that when the amount of CO₂ is doubled, the growth rate of microalgae increased to 75%. Douchal [10] stated that there exists a direct relationship between microalgae growth rate and carbon content.

To find out the effect of CO₂ on the growth rate of microalgae a culture was studied in batch photobioreactor for 12 days in temperature range of 25-27 °C with CO₂ concentrations of 0%, 10%, 20% and 30% mixed with air. Tests of samples were made on daily basis and results were examined for cell density versus each CO₂ concentration. As shown from the plots for four different values of CO₂ concentrations the growth of cells increases with increase in CO₂ concentrations. The other factors which also effect the growth such as light intensity, medium composition and mixing rate were kept constant.

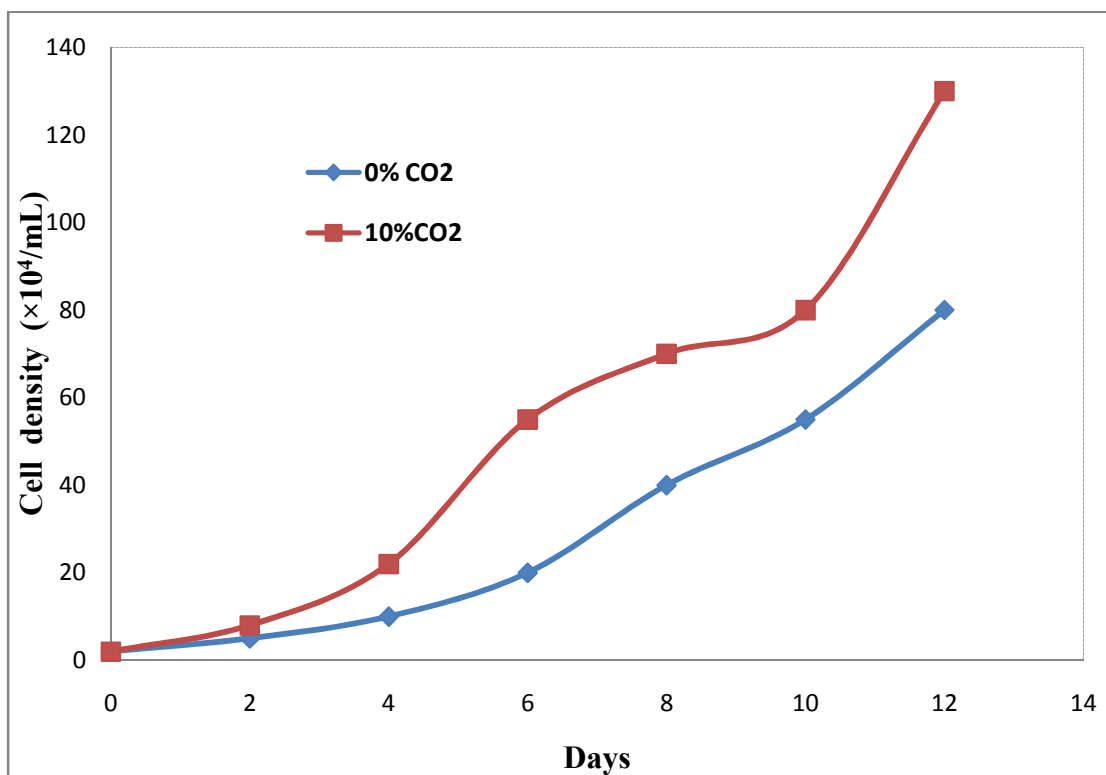


Fig.1 Microalgae growth with different CO₂ Concentration (vol %) in air.

The above figure shows that the microalgae cells growth rate is low with 0% CO₂ while with increase in the concentration of Carbon-dioxide (CO₂) from 0% to 10% the growth rate increases with time and reaches its maximum value on 12th day. Figure 2 shows the positive effect of carbon-dioxide concentration on the growth rate of microalgae. For the first two days the growth rate was almost the same at 20% CO₂ and 30% CO₂ concentrations.

From 4th day to 8th day the increase in growth rate for both concentrations of carbon-dioxide was linear. In the last two days of the experimental work, the number of cells increased more rapidly for 30% CO₂ compare to 20% CO₂ concentration.

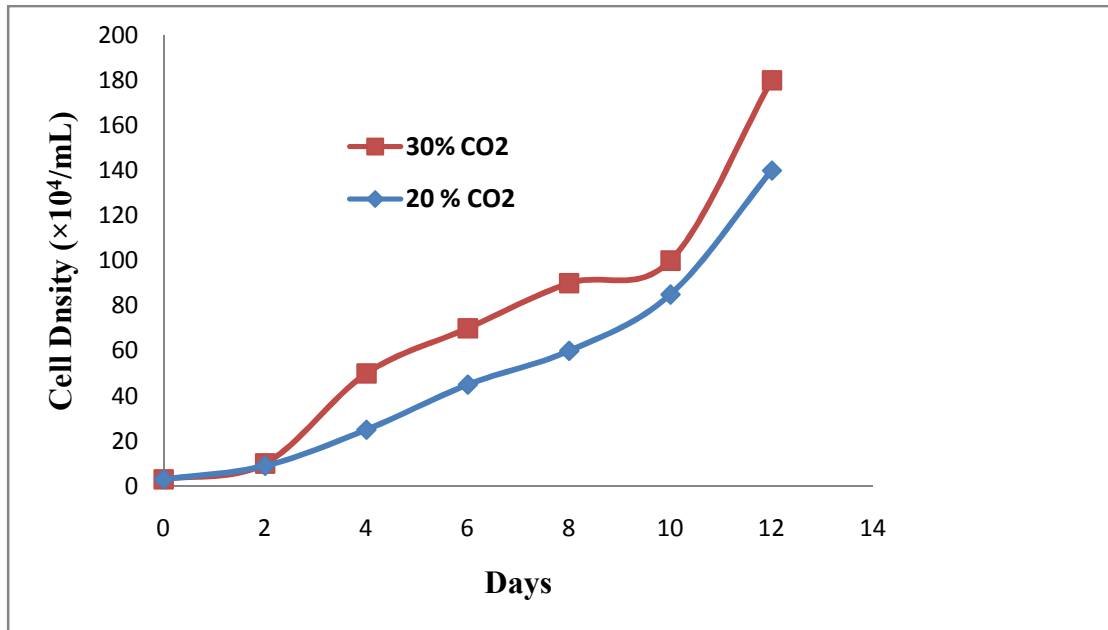


Fig.2 Microalgae growth with different CO₂ Concentration (vol %) in air.

Studies were performed to characterize the growth of microalgae. Figure 1 shows the growth rate of microalgae at 0% (v/v) and 10% (v/v) concentrations of CO₂. Without any CO₂ addition to the air the growth of microalgae was very slow by consuming CO₂ (0.035 % in air). The 10% (v/v) and 20% (v/v) of CO₂ (mixed with air) showed almost similar results with medium growth rates. For the concentration of 30% (v/v) the micro algal growth rate was higher as shown in figures 1 and 2.

4. Conclusions

This cultivation experimental system of microalgae shows the positive effect of carbon-dioxide on the cell growth rate. It shows that CO₂ dissolved in water could diffuse into the growth medium of the microalgae culture. The high concentration of CO₂ had a positive growth influence, as evident from the plots of cell density verses different carbon-dioxide concentrations. In addition, the growth system also shows that carbon-dioxide is the essential element for microalgae growth. It was also observed that the pH of the medium falls rapidly because, gaseous CO₂ dissolves in water and form carbonic acid with water when CO₂ gas is added. Moreover very high CO₂ flow rate is also unsuitable for micro algal growth. It is concluded that these microorganism possess a great potential to produce green fuels and solve the problems associated with the GHGs.

References

- [1] O. pulz, W. Gross, "valuable products from Biotechnology of Microalgae", *Applied Microbiology and Biotechnology*: 65 (2004), 635-648
- [2] L.Geong, 'M.Gillis.,Y.Hwang. "Carbon dioxide mitigation by Microalgal Photosynthesis".*Bulliten of the Korean chemical society*: 24 (2003) ,1763-1766
- [3]Chang, Chen, J.S.,Yeh, C.Y., K.L., Aisyah, R., D.J.,Lee, . " Cultivation, photo- bioreactor design and Harvesting of microalgae for bio-diesel production": a critical review, *Bio-resource Technology*



- (2011) 102: 71–81.
- [4] Chisti, “Biodiesel from microalgae”. *biotechnologyAdv* (2007) 25: 294-306.
- [5] G. Shelf, A. Sukenik, M.Green, Microalgae harvesting and processing”. A literature review, a Subcontract report technology research and development foundation ltd Haifa,Israel, August (1984).
- [6] A.Razzak, M.Ilyas, M.Hossain ‘effect of different ratio of air-CO₂ mixing feed on the growth of chlorella vulgaris and Nannochloropsis Oculata in batch photobioreactor’.
- [7] H.Gupta, L.S Fan., Carbonation and calcination cycle using high reactivity CaO for CO₂ separation from flue gas. *IndEngChem Res.* (2002) 41: 4035–4042.
- [8] Chang, Chen, J.S., C.Y. Yeh, K.L., Aisyah, R., D.J.,Lee, “ Cultivation, photo-bioreactor design and harvesting of microalgae for bio-diesel production”: a critical review.*Bio-resource Technology* (2011) 102: 71–81.
- [9] B.qiuan and K.Gao “Effects of CO₂ Enrichment on the bloom forming cyanobacteria” physiological responses and relationship with the availability of dissolved inorganic carbon (2002) 38 : 721-729
- [10] S. Douchal and Lyvansk, “Utilization of



Solving two-dimensional Poisson equation with nonlocal boundary conditions by meshless method

Masood Ahmad¹, Siraj-u-islam²

^{1,2} Department of Basic Sciences, University of Engineering & Technology, Peshawar, Pakistan, PO Box 814, Post code 25120

¹masood_suf@yahoo.com, ²siraj.islam@gmail.com

Abstract:

Various mathematical models that described real-world processes consist of partial differential equation (PDEs) with nonlocal boundary conditions. Second order parabolic PDEs with nonlocal boundary conditions have important applications in chemical engineering heat transfer phenomena and thermoelasticity. Therefore, interest in solving such PDEs numerically with nonlocal boundary condition has been growing fast. In this paper we consider two-dimensional Poisson equation with nonlocal boundary condition. We used meshless method based on Radial basis functions collocation technique along with splitting of shape parameter based on inverse multiquadric (CTWSPIMQ) for its numerical solution. We consider two examples of nonlocal boundary condition. One is two-point boundary condition and another is integral boundary condition. We paid attention to the influence of nonlocal boundary condition on the accuracy and condition number of the matrix arising in the numerical method.

Keywords: Meshless method, Condition number, Shape parameter, RBFs, Nonlocal boundary conditions, Poisson equation

1. Introduction

The formulation of nonlocal boundary value problem is necessary whenever the value of the unknown function is difficult to determined or impossible to find its value on the boundary. In nonlocal boundary condition the value of the unknown function on the boundary is connected with value of the unknown function inside of the given domain. Various prominent researchers have studied different types of PDEs with nonlocal boundary conditions arise in various problems in ecology, physics and biological sciences [1, 2, 3]. In paper [4], the author M. Dehghan considered one-dimensional heat equation with integral boundary condition. Similarly J. M. Vaqueroa and J.V. Aguiar also studied heat equation subject to nonlocal boundary condition [5]. The author, M. Siddique, studied two-dimensional diffusion equation subject to nonlocal boundary condition [6]. A thorough discussion on different nonlocal boundary value problems was reported in the literature and the reference therein [7,8,9,10].

Here, we considered two-dimensional Poisson equation of the form

$$-\frac{\partial^2 x}{\partial x^2} V(x, y) - \frac{\partial^2 y}{\partial y^2} V(x, y) = F(x, y), \quad 0 < x, y < 1. \quad (1)$$

Subject to

$$V(x, 0) = \beta_3(x), \quad V(x, 1) = \beta_4(x), \quad 0 \leq x \leq 1, \quad (2)$$



$$V(0, y) = \beta_1(y), \quad 0 \leq y \leq 1. \quad (3)$$

And on the boundary $x=1$, we considered two types of nonlocal boundary condition

a) Two-point boundary condition

$$V(1, y) = \alpha V(Y, y) + \beta_2(y), \quad 0 \leq y \leq 1, 0 \leq Y < 1 \quad (4)$$

b) Integral boundary condition

$$V(1, y) = \alpha \int_{\gamma_1}^{\gamma_2} V(x, y) dx + \beta_2(y), \quad 0 \leq y \leq 1, 0 \leq \gamma_1, \gamma_2 \leq 1 \quad (5)$$

$\beta_1(y)$, $\beta_2(y)$, $\beta_3(x)$, $\beta_4(x)$ and $F(x, y)$ are some given known functions and Y , γ_1 , γ_2 , α are real parameters. For $Y=0$, nonlocal boundary condition 4 and 5 reduce to Dirichlet boundary conditions.

2. Theory

2.1 Radial function

Let $\phi: R^S \rightarrow R$ is called radial function if there exists a univariate function $\phi: [0, 1] \rightarrow R$ such that

$$\phi(x) = \phi(r),$$

where $r = \|x\|$, and $\|\cdot\|$ is some norm on R^S . The generalized multiquadric (GMQ) is given as

$$\phi(r) = (1 + (cr)^2)^\beta,$$

where β , is any real number except non-negative integers [10]. The shape of GMQ RBF is controlled by two parameters (the exponent β and the shape parameter c). It is clear that Multiquadric (MQ), Inverse Multiquadric (IMQ) and Inverse Quadric (IQ) RBF are special cases of GMQ RBF. IMQ RBF is obtained by putting $\beta = -1/2$ in GMQ RBF. The parameter c is called shape parameter which controls the shape of the function.

2.2 The Method

Let us take $N + 1$ nodes along the x -direction such that $x_i = i \cdot dx$ where $dx=1/N$ and $i=0, 1, 2, \dots, N$. Similarly $M + 1$ nodes along the y -direction such that $y_j = j \cdot dy$ where $dy=1/M$ and $j=0, 1, 2, \dots, M$. Now split the shape parameter in Multiquadric RBFs is given as

$$IMQ = \left(\sqrt{1 + c_x(x - x_i)^2 + c_y(y - y_j)^2} \right)^{-1} \quad (6)$$

Now, from eq. (6) we can write

$$c_x = h \cdot N^2 \quad \text{and} \quad c_y = k \cdot M^2, \quad (7)$$

where k and h are some positive constants.

After this follow the procedure given in [10] in order to find the unknown function V for the problem given in eq. (1) to eq. (5). We denote the method given in [10] by CTWOSPIMQ.

3. Results and Discussions

Consider the problem given in Eq.1 with initial data given below

$$F(x, y) = 2 \cdot \pi^2 \cdot \sin(\pi \cdot x) \cdot \sin(\pi \cdot y),$$

$$\beta_1(y) = 0,$$

$$\beta_2(y) = -\alpha \cdot \sin(\pi \cdot \gamma) \cdot \sin(\pi \cdot y), \tag{8}$$

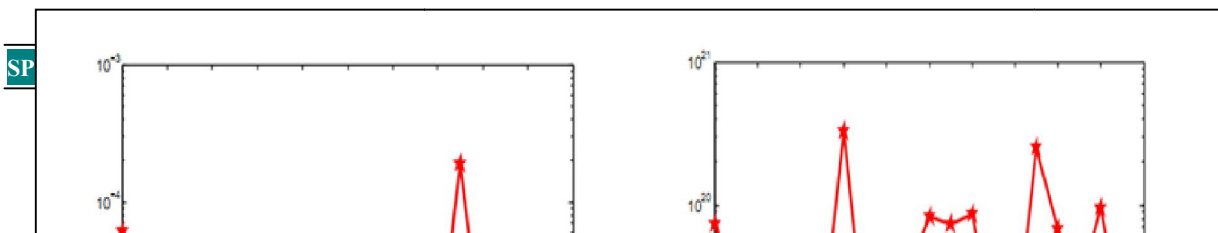
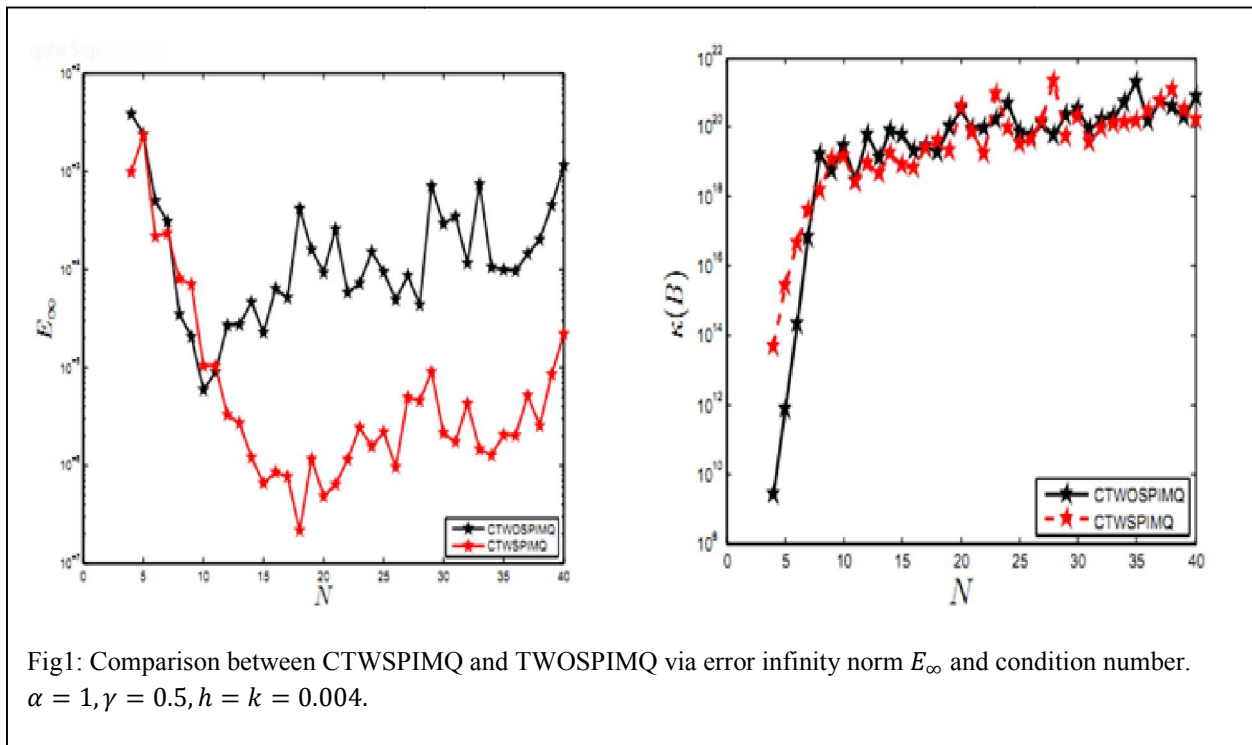
$$\beta_2(y) = -\alpha \cdot \sin(\pi \cdot y) \cdot (\cos(\pi \cdot \gamma_2) - \cos(\pi \cdot \gamma_1)) / \pi, \tag{9}$$

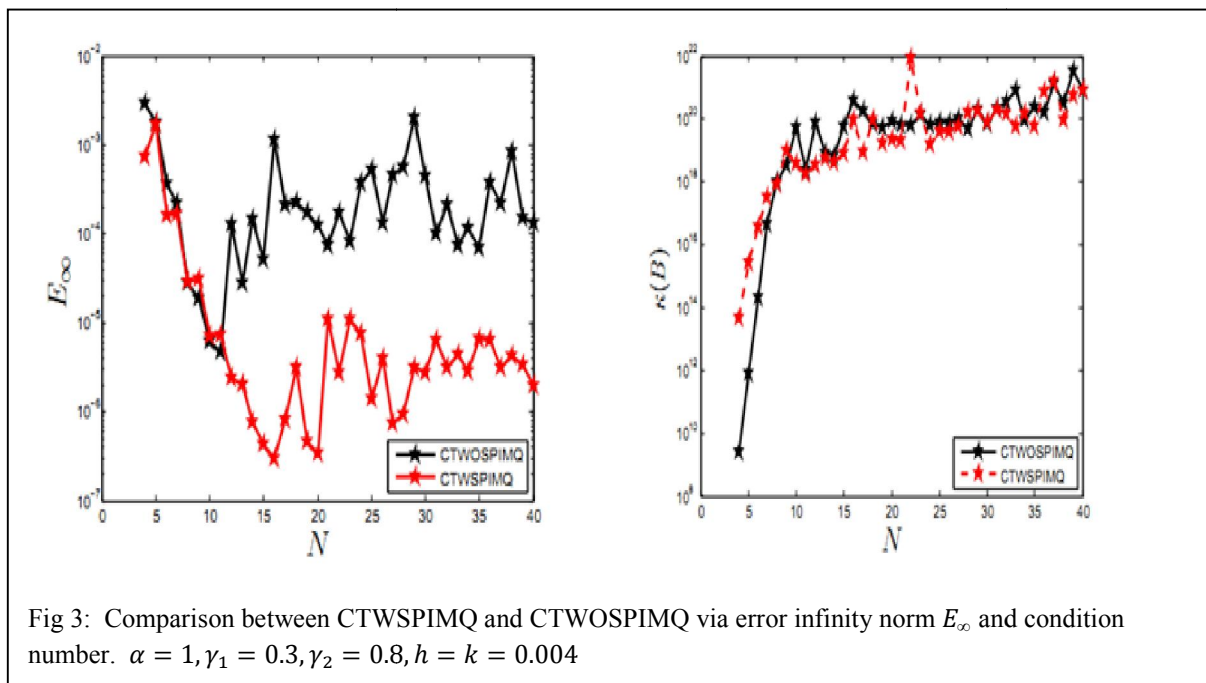
$$\beta_3(y) = 0,$$

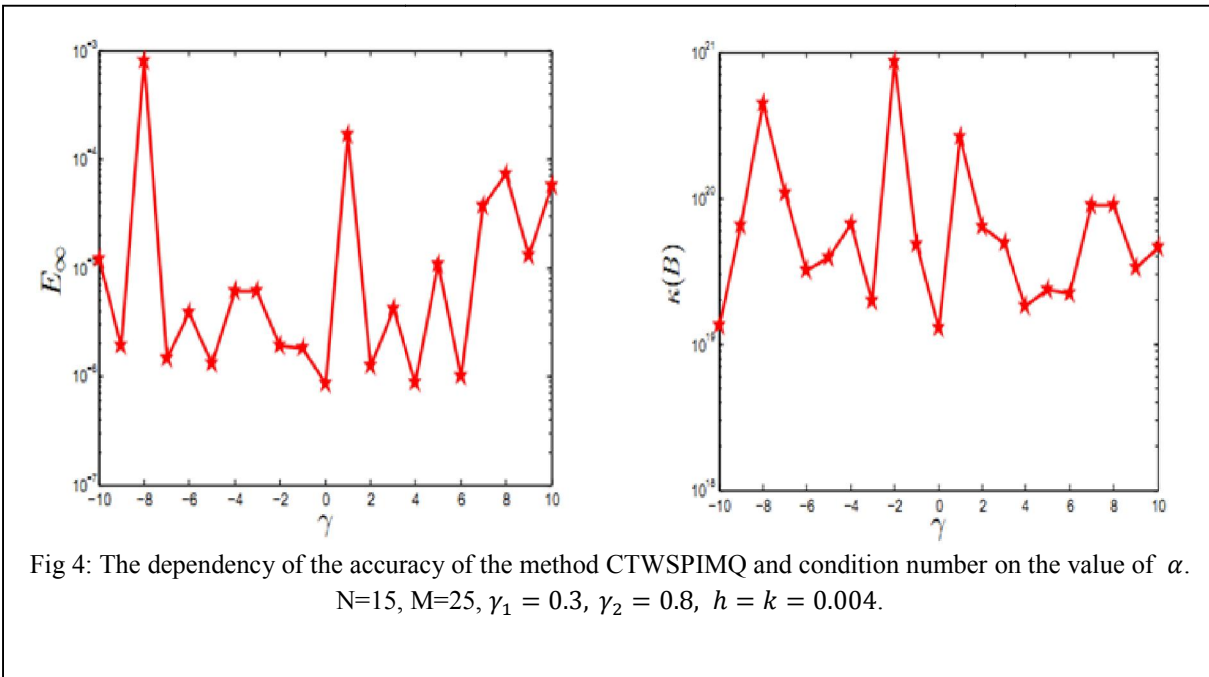
$$\beta_4(y) = 0,$$

The solution is

$$V(x, y) = \sin(x \cdot \pi) \cdot \sin(y \cdot \pi).$$







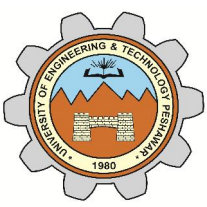
The results of the problem with two-point boundary condition (Eq. 4) are shown in fig (1) and (2). While the results of the problem with integral boundary condition (Eq.5) are shown in fig (3) and (4). In both cases the accuracy of the CTWSPIMQ become quite good for fine grid. The difference of the condition number of both the meshless methods also narrows down for fine grid.

4. Conclusions

In this paper the comparison of CTWSPIMQ and CTWOSPIMQ is performed. We conclude from the results given above that for refine grid the accuracy of the method CTWSPIMQ is quite good as compared to the method CTWPIMQ.

References

- [1] D. G. Eziani and G. A. Shvili. Investigation of the nonlocal initial boundary value problems for some hyperbolic equations. Hiroshima Mathematical Journal , 31:345-366, 2001.
- [2] G.Berikelashvili and N. Khomeriki. On a numerical solution of one nonlocal boundary-value problem with mixed Dirichlet-Neumann conditions. Lithuanian Mathematical Journal ,53:367-380, 2013.
- [3] Ruyun Ma. A survey on nonlocal boundary value problems. Applied Mathematics E-Notes ,7:257 {279, 2007.
- [4] M. Dehghan. The one-dimensional heat equation subject to a boundary integral specification. Chaos, Solitons and Fractals , 32:661-675, 2007.
- [5] J. M. Vaqueroa and J.V. Aguiar. On the numerical solution of the heat conduction equations subject to nonlocal conditions. Applied Numerical Mathematics, 59:2507-2514, 2009.
- [6] M. Siddique. Smoothing of cranknicolson scheme for the two dimensional diffusion with an integral condition. Applied Mathematics and Computation , 214:512-522, 2009.
- [7] A. Taherpour and A. Hosseinpour and L. Abasabadi and A. Hosseinpour. The solve of laplace equation with nonlocal and derivative boundary conditions by using non polynomial spline. American Journal of Engineering Research (AJER), 2:76-78, 2013.



[8] W.T. Ang. A method of solution for the one-dimensional heat equation subject to nonlocal condition. South Asian Bulletin of Mathematics, 26:185-191, 2002.

[9] K.J. Hayman B.J. Noye. Explicit two-level finite difference methods for the two-dimensional diffusion equation. International Journal of Computer Mathematics, 42:223-236, 1992.

[10] S.Sajavicius. Optimization, conditioning and accuracy of radial basis function method for partial differential equations with nonlocal boundary conditions a case of two-dimensional poisson equation. Engineering Analysis with Boundary Elements, 37:788-804, January 2013.



Conference Proceedings SPI 2014 [45-49]

Review of Process Simulation and Simulation Software-Open Source Software Development

Muhammad Shoaib^{1,a}, Walter Wukovits², Saeed Gul³

^{1,3}Department of Chemical Engineering, University of Engineering and Technology, Peshawar, Pakistan.

²Institute of Chemical Engineering, Vienna University of Technology, Vienna Austria

¹engr.shoaibjadoon@gmail.com, ³saeedgul@nwfpuet.edu.pk, ²walter.wukovits@tuwien.ac.at

Abstract:

Process simulation has been emerging as a growing field and inevitable demand of process industry in 21st Century. In the shadow of this ultimate need, several options are emerging to be useful in this regard. Among various simulation software there also are emerging open source freely available software to aid the existing proprietary ones in this regard. The development of these software and the CAPE-OPEN standards that lay down the principles of their application and usage are the parts of this study.

Keywords: Simulation, Simulation Software, CAPE-OPEN Standard

1. Introduction

Research over last 50 years or more has led to a number of areas where a massive development has taken place. Simulations with models comprising some millions and billions of algebraic or differential equations (either two-space dimensional or three dimensional) are to be solved in actual process calculations of material and energy balances [8]. Process simulation deals mainly with the design, development, analysis and optimization of any technical process [10]. Chemical engineers utilize chemical process simulation to design or retrofit complex process facilities. By means of Chemical Process Simulation software, chemical engineers can determine the overall effects of the changes to be made in one particular area in a process, predict capital cost expenditures, follow process emissions, and analyze optimization and integration options [3] as shown in fig. 1.

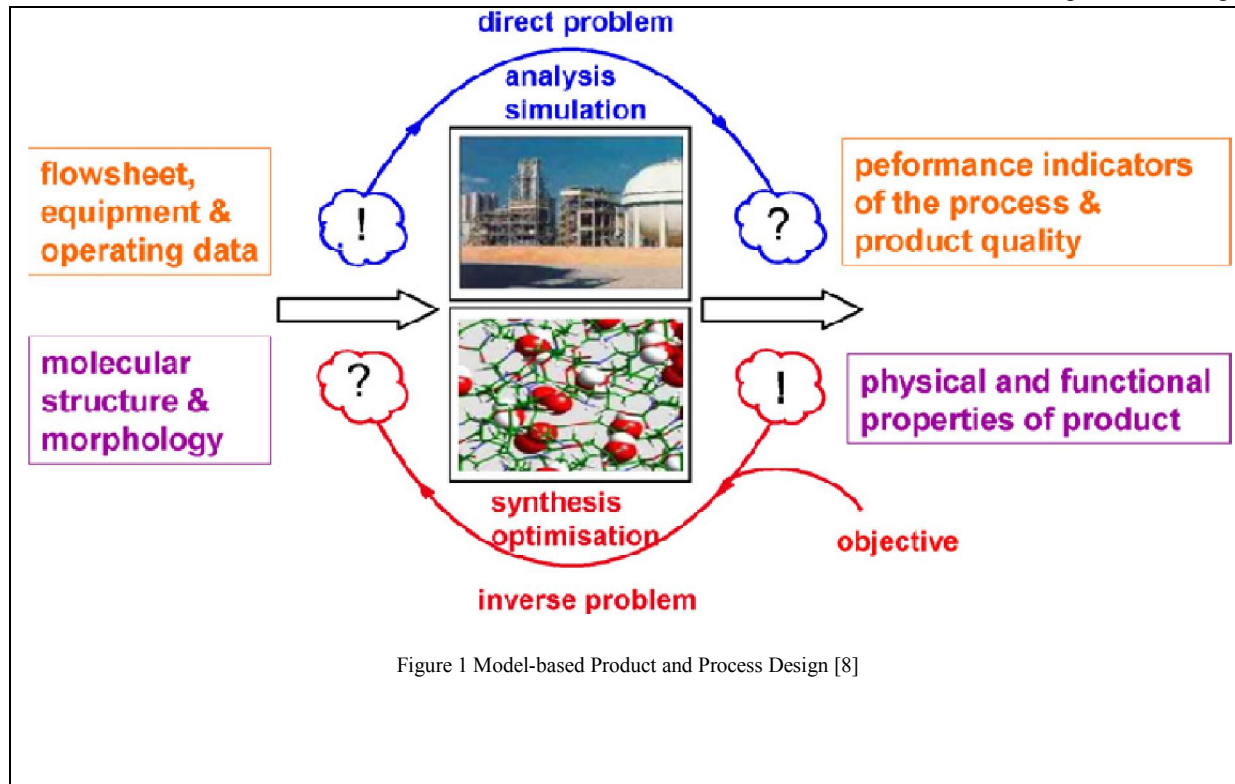


Figure 1 Model-based Product and Process Design [8]

At present commercial chemical engineering process simulators used mainly in industry are; Aspen plus, Hysys, ProSim, WinSim, PRO/II and ChemCAD which are used in all sectors and areas of a process. It was established in 1980s that tremendous progress had taken place till that time in the development of chemical process simulators. The major improvement in the simulation technology came with the advent of “Sequential Modular Simulator” [11].

The reasons lying behind their wide adaption are; fluid data handling capabilities, component database and physical property database and an easy to use graphical user interface for unit operations and process flowsheet solutions [9].

Process simulation software may either be open source or closed source. Open source software are freely available to the users without any cost, having source code available to the users. The details of this distinctive feature are described well by Wheeler in 2005 in his paper on open source software. Closed source software are commercial (proprietary) software which have a license owned by the originators and it is not free software.

From the perspective of economics, it is said that open source software have been an innovative tool in the process industry. It is a new way of producing software based on an unconstrained access to the source code [2].

2. Development of Simulation Software

The first few years of academic research in the 1950s and 1960s was largely focused on mathematical modeling, simulation and optimization to design selected unit operations. The early work was exemplarily exploring the



potential of mathematical analysis and numerical algorithms implemented on a computer to deal with the mathematical complexity of the nonlinear and fairly large process models. Emphasis was not only on individual unit operations like adsorption (Acrivos, 1956; Amundson, 1948), distillation (Acrivos & Amundson, 1953; Amundson & Pontinen, 1958; Mah, Michaelson, & Sargent, 1962) or chemical reactors (Aris, 1960; Blakemore & Aris, 1962; Davidson & Shah, 1965; Gilles & Hofmann, 1961; Youle, 1961) but also on complete processes (Brambilla, et al, 1971; Frank & Lapidus, 1966) [8].

The models were surprisingly sophisticated and covered spatially (Gilles, Lubeck, & Zeitz, 1970) as well as substantially (Valentas & Amundson, 1968; Zeman & Amundson, 1965) distributed systems. These new methods were recognized to help substituting crude design heuristics and avoiding time-consuming manual calculation procedures [8].

The process simulator has today become a standard tool in the repertoire of process engineers. The main advantageous aspect that boosted the importance of process simulators are; various process modifications can be evaluated using standard software packages such as; CHEMCAD, Aspen Plus, HYSYS, PRO/II and gPROMS in a short time without the need for extensive pilot plant experimentation [7]. It has been recognized since early 1960s that process simulation is quite useful tool for the process design, analysis and optimization activities. The development in this regard continued till 1995, when CAPE-OPEN Program begun. It was in 1997, the CAPE-OPEN Standard was given a proper formulation and the open source free software were also introduced. Interest in Process Simulation and CAPE-OPEN architecture is based on its possible means to access the information contained within the simulation in a reliable and consistent way [1].

The list of commonly used process simulation software includes; Aspen plus, Pro/II, ProSim Plus, Hysys, ChemCAD, MASSBAL, WinGEMS (pulp and paper), FlowMac (pulp and paper), Solvo (energy, power and heat), COCO (free cape open compliant steady state simulation software/environment), LIBPF (LIBRARY for process flowsheeting in C++), and DWSIM (an open source chemical process simulator) [8].

3. CAPE-OPEN Standard

The CAPE-OPEN (CO) standard allows users to have a suitable environment for the development of software through open source free software development pathway. CAPE-OPEN is developing to be a commonly used integration tool being applied in the modern industry. The CAPE-Open (CO) standards are uniform set of rules applied to interface the process modeling software components developed especially for the design and development of a chemical process. They are described and presented in the form of a formal documentation set (CAPE-Open standards and supporting documents) put forward by CAPE-OPEN Laboratories Network (CO-LaN) [6].

The CAPE-OPEN standard allows the implementation of thermodynamic models and unit operations in simulation tools. For calculations of thermodynamic properties, the CAPE-OPEN standard has defined the Property Package interface. It is a collection of methods and compounds for calculating any of a set of physical properties for the different phases of a mixture or a pure compound [4]. The standard enables communication between a process

modeling environment and process modeling components by defining an interface named Material Object. This interface allows the exchange of information like pressure, temperature, flow or composition between simulation tools and external components [5]. The information storage takes place in CAPE-OPEN flowsheeting environment allows the process to be represented and solved as shown in fig.2.

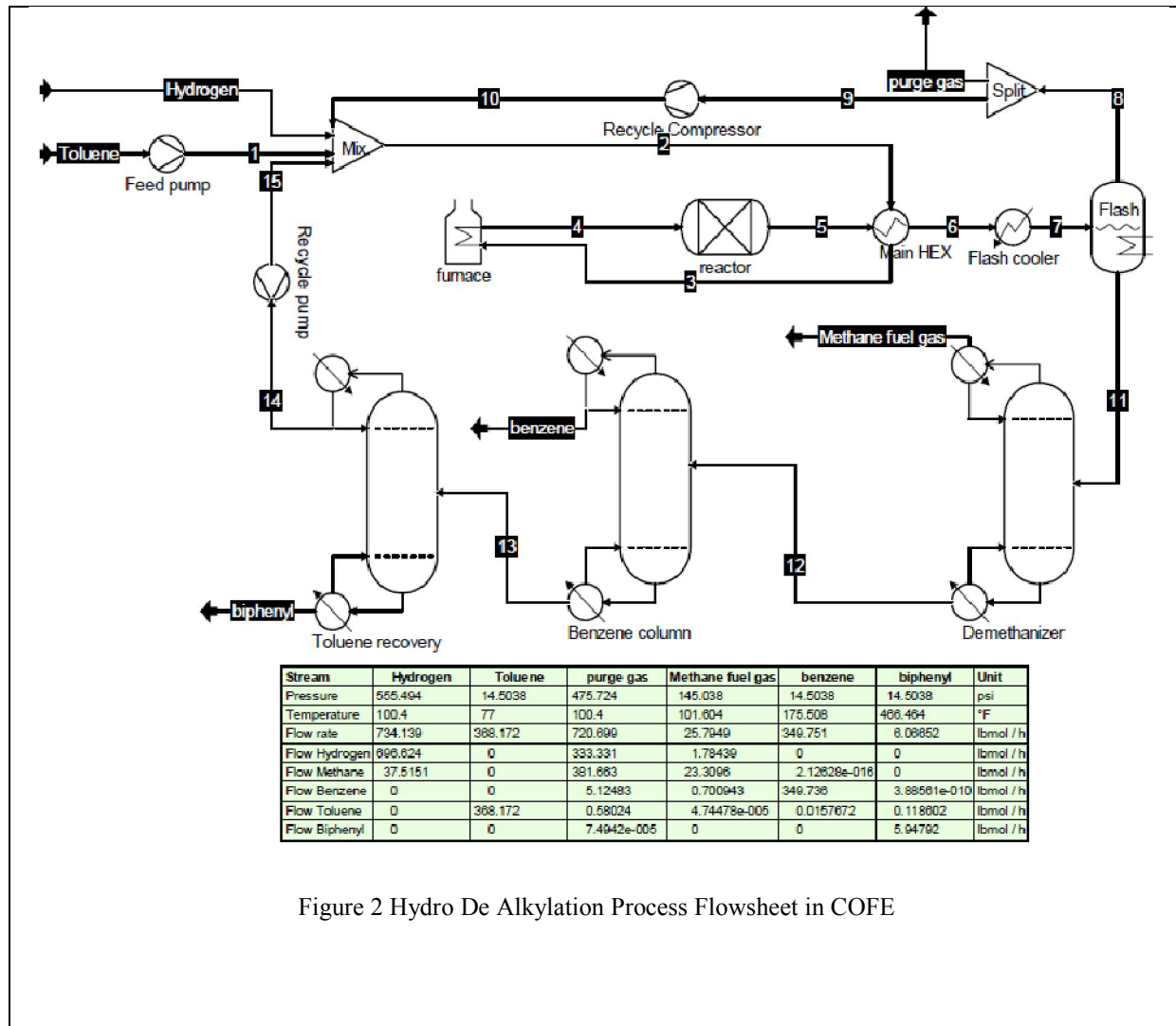


Figure 2 Hydro De Alkylation Process Flowsheet in COFE

4. Conclusion

It can be concluded that software development is a continuous process and is taking place throughout the world to effectively enhance the capabilities of software to provide users with more advanced and well developed features of the software they may use, either open source or closed source. The main focus is directed here towards the open source software for process simulation because these are the software that provide users with the availability of source code so that that user may modify, re-distribute or use it with complete freedom. This freedom of usage and modification makes them helpful in the learning aspects of process simulation.



References

- [1] Barrette Jr., W. a.. Development of a chemical process modeling environment based on CAPE-OPEN interface standards and the Microsoft .NET framework. *Computers and Chemical Engineering* , (2005), 191-201.
- [2] Bonaccorsi, A. a.. Why Open Source software can succeed. *research policy*32 , (2003), 1243–1258.
- [3] Casavant, T., Using Chemical Process Simulation to Design Industrial Ecosystems. *Journal of Cleaner Production* 12 , 901-908, (2004).
- [4] CO-LaN, Cape-Open interface specifications thermodynamic and physical properties version 1 , (2002).
- [5] Dauber, F. Achieving higher accuracies for process simulations by implementing the new reference equation for natural gas. *Computers and Chemical Engineering*, (2011), 15-21.
- [6] Domancicha, A. a. b. Systematic generation of a CAPE-OPEN compliant simulation module from GAMS and FORTRAN models. *Chemical Engineering Research and Design*, 8 , (2010), 421-429, (2010).
- [7] Halim, I., & Srinivasan, R. A knowledge-based simulation-optimization framework and system for sustainable process operations. *Computers and Chemical Engineering* , 35, (2011), 92-105).
- [8] Klatt, K., & Marquardt, W. Perspectives for process systems engineering—Personal views from academia and industry. *Computers and Chemical Engineering* , 33, (2009), 536–550.
- [9] Madhusudana, R., Rengaswamy, R., & Suresh, A. a. (2004), Industrial Experience With Object-Oriented Modelling FCC Case Study. *Chemical Engineering Research and Design* , (2004), 527-552.
- [10] Rhodes, L. The Process Simulation Revolution: Thermophysical Property Needs and Concerns. *Chem. Eng. Data* , . (1996), 947-950.
- [11] Stephanopoulos, G., & Reklaitis, G. (2011). Process systems engineering: From Solvay to modern bio- and nanotechnology. *Chemical Engineering Science* , 66, (2011), 4272–4306.



Conference Proceedings SPI 2014 [50-55]

Meshless based complex quadrature solution for highly oscillatory integrals and the integrals having no stationary points

Uzma Nasib¹, Siraj-ul-Islam²

^{1,2}Department of Basic Sciences, University of Engineering and Technology, Peshawar, Pakistan.

¹uzminasib2013@gmail.com, ²siraj-ul-islam@nwfpuet.edu.pk

Abstract:

The exact solution of High Oscillatory Integrals (HOIs) and integral having no stationary points is difficult to obtain. So, an alternate way is to use numerical techniques, for such problems. In this paper an efficient method, based on Modified Levin approach is employed for such problems. In the proposed technique multiquadric radial basis function (MQRBF) is replaced by Bessel radial basis function (BRBF). In this scheme the integration problems are first transformed into their corresponding ODEs or PDEs form, and then the numerical simulations of the corresponding ODEs or PDEs are performed.

Keywords: Meshless method, Oscillatory integral, Levin's method, Shape parameter, Condition number, Radial Basis function, Bessel RBF.

1. Introduction

Computational scientists and mathematicians showed their attention towards efficient and accurate numerical methods and challenges encountered in the evaluation of HOIs. HOIs have various applications which occur in quantum mechanics, electromagnetic waves, optics and acoustics and their calculation is one of the key research problem [1, 2, 3].

The above mentioned HOIs are uniformly represented as

$$I = \int_a^b f(x) e^{i\omega g(x)} dx \quad (1)$$

where $f(x)$ is called amplitude, $g(x)$ phase function, $f(x)$ and $g(x)$ are both smooth functions. The parameter $\omega \rightarrow 0$ called frequency parameter, is a positive real number in the given interval $[a, b]$. The integrand given in Eq.(1) may or may not have stationary points. In the case of stationary points of Eq.(1) $g'(x)=0$ in $[a, b]$.



The methods specific for HOIs are categorized into two main groups, Levin's type of method [4] and Filon type of method [5]. The former converts the oscillatory integrals into ODEs or PDEs by using monomial basis in a collocation method. The later is based on asymptotic theory.

We construct meshless methods based on Levin's approach for the HOIs, without critical points in the interval of integration [a, b]. The procedures are effective if the frequency of HOIs is very high. However its efficiency is effected if the oscillatory integral contains critical points in interval [a, b]. Different RBFs have been used effectively for univariate or bivariate interpolation of uniform and scattered data, both for regular or irregular geometries.

The coefficient matrix, resulted after discretizing PDEs, is dense and often ill-conditioned. The major stumbling block in the use of MQRBF is the ill-conditioned coefficient matrix, which badly hampers the accuracy of the underline algorithm. To overcome this difficulty, the authors have proposed oscillatory radial basis functions in [6] given by

$$\varphi(r) = \frac{J_{\frac{d}{2}-1}(c.r)}{(c.r)^{\frac{d}{2}-1}} \quad d=1, 2, 3, \dots \quad (2)$$

Where J_{α} represents the J Bessel function of order α .

The paper is organised as follows: In section 2, the meshless method (MM) based on different type of RBFs is described. In section 3, test problem and discussion is given. In section 4, some conclusion is given.

2. Meshless Method

A univariate continuous function, defined for r which is a positive real number, may or may not have a free parameter called an RBF $\varphi(r)$. The free parameter is called the shape parameter of the RBF, where c is used for shape parameter. The following form is used for an RBF interpolant, for a set of M centers x_1^c, \dots, x_M^c , given in R^d .

$$P(x) = \sum_{i=1}^M \gamma_i \varphi(\|x - x_i^c\|_2, c), \quad x \in R^d. \quad (3)$$

The interpolation condition

$$P(x_k) = f_k, \quad k=1, 2, \dots \quad (4)$$

is used for the evaluation of the coefficients γ_i , $i=1, \dots, M$. In this case we take $M=N$.

The following linear system will be solved to obtained the coefficients γ_i , $i=1, \dots, M$.

$$D\gamma = f, \quad (5)$$

the interpolant matrix, which is known as D , is an $M \times M$ matrix having values.

$$D = \varphi_{ij} = \varphi(\|x_j - x_i^c\|), \quad i, j=1, 2, \dots, M. \quad (6)$$



Here we propose the Bessel radial basis function (BRBF) of orders 5, 7 and 9 and instead of monomials and MQRBF.

BRBF of order 5 (BRBF5) can be written as:

$$\varphi(r) = \sqrt{\frac{2}{\pi}} \left[\frac{\sin(c.r) - (c.r)\cos(c.r)}{(c.r)^3} \right], \quad (7)$$

BRBF of order 7 (BRBF7) is given as:

$$\varphi(r) = \sqrt{\frac{2}{\pi}} \left[\frac{3\sin(c.r) - 3(c.r)\cos(c.r) - (c.r)^2\sin(c.r)}{(c.r)^5} \right], \quad (8)$$

BRBF of order 9 (BRBF9) can be written as:

$$\varphi(r) = \sqrt{\frac{2}{\pi}} \left[\frac{15\sin(c.r) - 15(c.r)\cos(c.r) - 6(c.r)^2\sin(c.r) + (c.r)^3\cos(c.r)}{(c.r)^7} \right], \quad (9)$$

MQ basis function is given as follows:

$$\varphi(r) = \sqrt{c^2 + r^2}, \quad (10)$$

where $r^2 = (x - x_k)^2$, $k=1, 2, \dots, M$ and c is the shape parameter.

For solving the oscillatory integrals, given in Eq. (1) we use the function $P(x)$ which satisfies the following ODE:

$$f(x) = P'(x) + i\omega g'(x)P(x). \quad (11)$$

The above equation is attained by putting Eq.(11) into Eq.(1)

$$\begin{aligned} I_l &= \int_a^b [P'(x) + i\omega g'(x)P(x)] e^{i\omega g(x)} dx \\ &= \int_a^b \frac{d}{dx} [P(x)e^{i\omega g(x)}] dx \\ &= P(b)e^{i\omega g(b)} - P(a)e^{i\omega g(a)} \end{aligned} \quad (12)$$

In finding numerical solution of solving Eq.(11) is the selection of proper basis functions, having better approximating properties. So, for obtaining numerical solution of Eq.(11) Levin [4] has used monomial basis. The rest of the procedure is same to [7]. For derivatives of $P(x)$, the RBFs approximation can be written as

$$LP(x) = \sum_{i=1}^M \gamma_i L\varphi(r, c) \quad (13)$$

where L is the first-order derivative operator.

Using the nodal points, the coefficients γ_i , $i=1, 2, \dots, M$ can be found in the following form:

$$\begin{bmatrix} \varphi'_{11} + i\omega g'(x_1)\varphi_{11} & \varphi'_{12} + i\omega g'(x_1)\varphi_{12} & \cdots & \varphi'_{1M} + i\omega g'(x_1)\varphi_{1M} \\ \varphi'_{21} + i\omega g'(x_2)\varphi_{21} & \varphi'_{22} + i\omega g'(x_2)\varphi_{22} & \cdots & \varphi'_{2M} + i\omega g'(x_2)\varphi_{2M} \\ \vdots & \vdots & \ddots & \vdots \\ \varphi'_{M1} + i\omega g'(x_M)\varphi_{M1} & \varphi'_{M2} + i\omega g'(x_M)\varphi_{M2} & \cdots & \varphi'_{MM} + i\omega g'(x_M)\varphi_{MM} \end{bmatrix} \begin{bmatrix} \gamma_1 \\ \gamma_2 \\ \vdots \\ \gamma_M \end{bmatrix} = \begin{bmatrix} f(x_1) \\ f(x_2) \\ \vdots \\ f(x_M) \end{bmatrix} \quad (14)$$



In matrix form, it can be expressed as:

$$\phi\gamma = F, \quad (15)$$

where

$$F(x) = [f(x_1) \quad f(x_2) \quad \dots \quad f(x_M)]^t,$$

$$\gamma = [\gamma_1 \quad \gamma_2 \quad \dots \quad \gamma_M]^t,$$

and

$$\phi_{st(MQRBF)} = \frac{r}{\sqrt{c^2+r^2}} + i\omega g'(x_s)\sqrt{c^2+r^2}. \quad (16)$$

$$\phi_{st(BRBF5)} = \sqrt{\frac{2}{\pi}} \mathcal{C} \left[\frac{\sin(c.r)}{(c.r)^2} - \frac{3(\sin(c.r) - (c.r)\cos(c.r))}{(c.r)^4} \right] + i\omega g'(x_s) \sqrt{\frac{2}{\pi}} \left[\frac{\sin(c.r) - (c.r)\cos(c.r)}{(c.r)^3} \right]. \quad (17)$$

$$\phi_{st(BRBF7)} = \sqrt{\frac{2}{\pi}} \mathcal{C} \left[\frac{6(c.r)\sin(c.r) - (c.r)^2\cos(c.r) + 15\cos(c.r)}{(c.r)^5} - \frac{15\sin(c.r)}{(c.r)^6} \right] + i\omega g'(x_s) \sqrt{\frac{2}{\pi}} \left[\frac{3\sin(c.r) - 3(c.r)\cos(c.r) - (c.r)^2\sin(c.r)}{(c.r)^5} \right]. \quad (18)$$

$$\phi_{st(BRBF9)} = \sqrt{\frac{2}{\pi}} \mathcal{C} \left[\frac{45\sin(c.r) - 10(c.r)\cos(c.r) - (c.r)^2\sin(c.r)}{(c.r)^6} + \frac{105\cos(c.r)}{(c.r)^7} - \frac{105\sin(c.r)}{(c.r)^8} \right] + i\omega g'(x_s) \sqrt{\frac{2}{\pi}} \left[\frac{15\sin(c.r) - 15(c.r)\cos(c.r) - 6(c.r)^2 + (c.r)^3\cos(c.r)}{(c.r)^7} \right]. \quad (19)$$

is the st^{th} matrix element of the $M \times M$ matrix ϕ .

Truncated singular value decomposition (TSVD) is highly recommended in MQRBF, when the system is bad-conditioned. In TSVD procedure, the accuracy of the method gets lower when the rows corresponding to singular values are eliminated.

TSVD is not recommended in our present work based on BRBF, because the resulting matrices are well-conditioned.

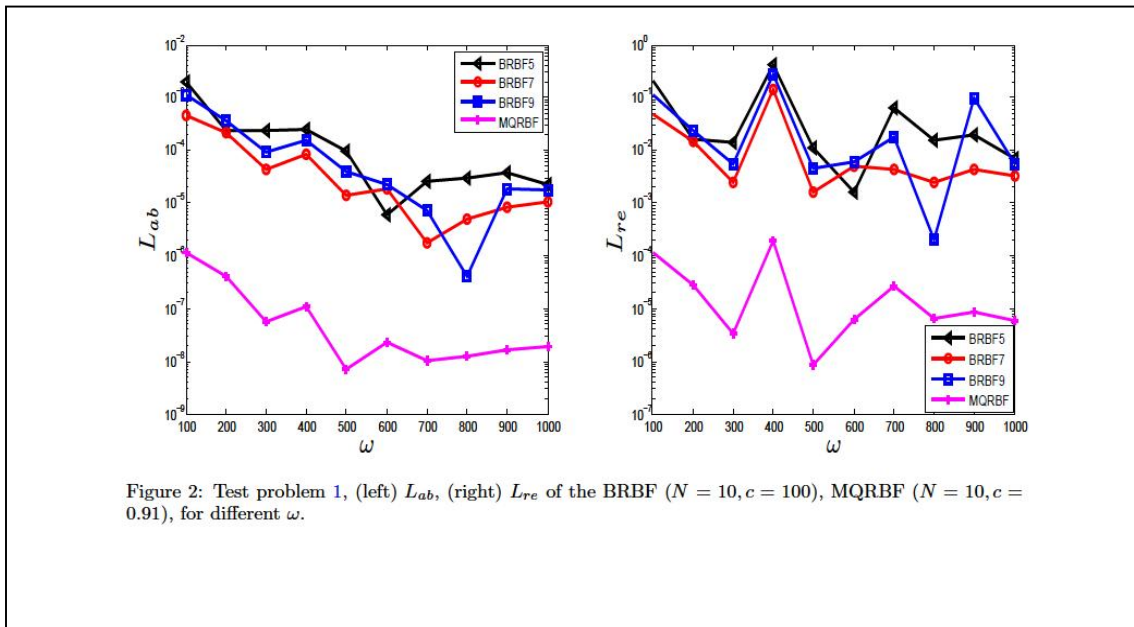
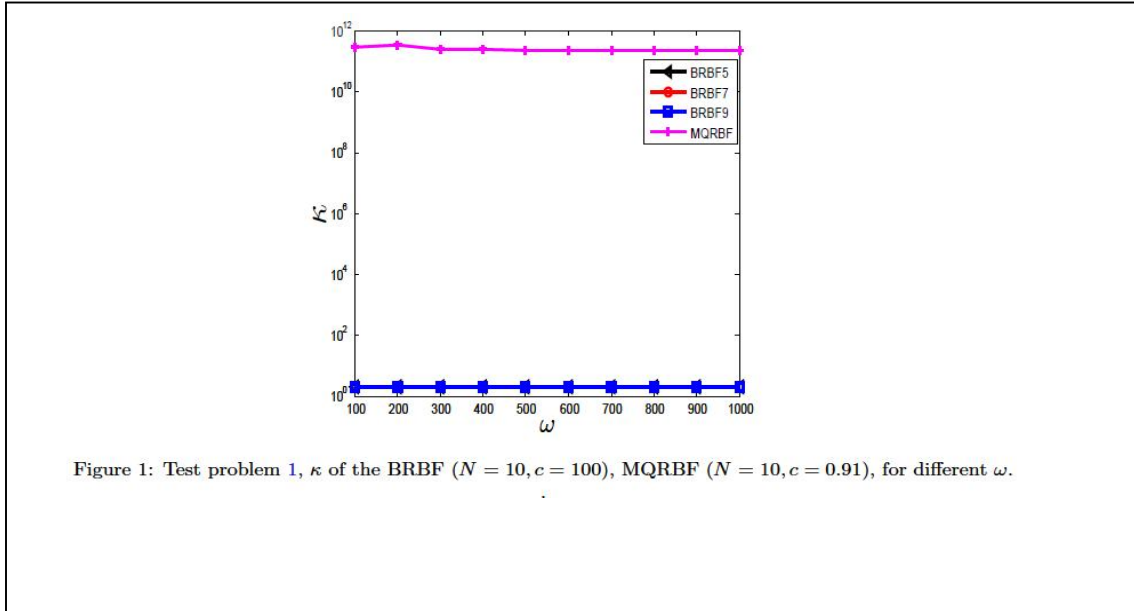
3. Results and Discussions

3.1 Test problem

$$I = \int_0^1 \left[\frac{1}{x+1} e^{\frac{i\omega}{\sqrt{x^2+2x+2}}} dx \right] dx$$

Numerical results of the test problem (1) are shown in Figs. 1-2. The above oscillatory integral has been mentioned in [8]. In this problem, the performance comparison of the condition number (K) the BRBF5-BRBF9 and MQRBF based meshless methods, are shown in Fig.1.1. The coefficient matrices of the BRBF5-BRBF9 based meshless methods are well-conditioned where, as system matrices of the MQRBF based meshless method is ill-conditioned.

Accuracy wise, the absolute L_{ab} and relative L_{re} error norms of the BRBF5-BRBF9 are not as good as the MQRBF for different values of ω and fixed number of collocation points i.e. $N=10$, as shown in the Fig. 1.2. The order of accuracy of the L_{ab} error norm of the MQRBF is order (10^{-9}) and that of the BRBF is order (10^{-7}).



The MQRBF based MM produces a good accuracy of L_{ab} and L_{re} error norms with bad conditioned numbers. The BRBF5-BRBF9 based meshless methods produce reasonably good accuracy but lower than the MQRBF, but due to lower order of its condition number it becomes valuable.



References

- [1] Miks A., Novak J., and Novak P., Method for numerical integration of rapidly oscillating functions in diffraction, *Int. J. Numer. Meth. Eng.* 26 (2006), 27-213.
- [2] Garcia-Martnez L., Rosete-Aguilar M., and Garduno-Mejia J., Gauss-legendre quadrature method used to evaluate the spatio-temporal intensity of ultrashort pulses in the focal region of lenses, *Appl. Optic.* 51 (2012).
- [3] Wu Y. M., Jiang L. J., and Chew W. C., An efficient method for computing highly oscillatory physical optics integrals, *Prog. Electromagn. Res.* (2012), 127-211.
- [4] Levin D., Procedures for computing one and two-dimensional integrals of functions with rapid irregular oscillations, *Math. Comp.* 158 (1982), 531-538.
- [5] Filon L.N.G., On a quadrature formula for trigonometric integrals, *Proc. R. Soc.* 49 (2005), 38-47.
- [6] Fornberg B., Larsson E., and Wright G., A new class of oscillatory radial basis functions, *Math. Comp. with Applic.* 51 (2006), 1209-1222.
- [7] Siraj-ul-Islam, Al-Fhaid A.S., and Zaman S., Meshless and wavelets based complex quadrature of highly oscillatory integrals and the integrals with stationary points, *Eng. Anal. Bound. Elem.* 37 (2013), 136-1144.
- [8] Harris P.J. and Ke Chen, An efficient method for evaluating the integral of a class of highly oscillatory functions, *J. Comp. Appl. Math.* 230 (2009), 433-442



Conference Proceedings SPI 2014 [56-62]

Modeling and Simulation of Osmotic Distillation Process of Fruit Juice Concentration

Sher Ahmad¹, Dr. Muhammad Younas²

^{1,2}Department of Chemical Engineering, University of Engineering and Technology, Peshawar, Pakistan.

^asheruet@gmail.com, ^benr_unas@nwfpuet.edu.pk

Abstract:

The demand for fruit juices with high quality rather than the whole fruits has been increasing day by day. Fresh fruit contains more than 80 % of water which makes the transportation and storage uneconomical. Concentration of liquid foods in general and fruit juices in particular to high concentration up to 70-80%, will remove high amount of water. This will reduce packing and transportation costs. Storage and handling will be reduced as well. And more importantly concentrates will be preserved for longer period of time.

Conventional Techniques used for fruit juice concentration have disadvantages in one way or another. Another emerging technique for juice concentration is osmotic distillation process. It gives high concentration with better quality than other conventional techniques, like reverse osmosis and evaporation.

In this research work, the model for water transport flux prediction is developed in hollow fiber, hydrophobic membrane, using resistance in series approach. Feed (sucrose) was taken in fibers while osmotic agent (CaCl₂) was taken in shell side. In this study Knudsen flow was dominated because of the pore size of the membrane. The developed model was then simulated using MATLAB. In this study CaCl₂ Concentration was varied from 2M-6M and the effect of varying concentration on water flux was studied. The flux obtained was from 1.5kg/m²hr-3.5kg/m²hr. The Predicted water flux obtained from the simulation results was then validated with experimental data from literature. Finally, the effect of different parameters on water flux was studied.

Keywords: Osmotic Distillation, Osmotic Agent, Membrane Contactor, Hydrophobic, Microporous

1. Introduction

The demand for fruit juice is increasing day by day all over the world. However rapid degradation of natural ingredients, transportation and storage of fruit juices in bulk makes the process uneconomical [1].

Concentration of fruit juice can make the process economical by removing 60-70% of water, which will reduce its transportation and storage costs up to high extent. Also preservation of juices can also be done by storing its concentrate rather than in bulk form, because concentrates are more inert to spoilage. So from this fact, to develop best concentration techniques with low cost and high quality concentrate is of prior need [2, 3].



In recent past, different techniques have been used for fruit juice concentration in the industry like vacuum evaporation, Reverse osmosis and freeze concentration. However all of these techniques have some shortcomings that do not fulfill the demands for better quality fruit juices with low cost [4].

Vacuum evaporation concentration is one of the oldest and well established techniques, used in food industry. But since in this technique phase changes are involved due to heating so high energy consumption and degradation of thermo-sensitive components are the major drawbacks of this technique. Energy recovery systems are required in order to reduce energy consumption but that drastically increase the capital cost up to 300% [5].

Freeze Concentration is another well-known technique that gives high quality of concentrates as it works at low temperature. But due to low final concentration (45-50%) and very high capital cost its application is still limited [6].

Reverse Osmosis (RO) is a membrane base technique for efficient concentration of fruit juice up to 25%. It's capital and operation cost is lower comparing to evaporative and freeze drying concentration. But the main problem with RO is that is impracticable and economical when concentrating juices above 30% and economical due to high osmotic pressure and fouling problem [7].

Osmotic distillation process has gained a lot of interest in recent past, due to its ability of producing high quality concentrates [1].

Literature indicated that Osmotic Distillation is used to concentrate fruit juices up to 75% with high quality [2, 6]. Moreover, Osmotic distillation process being operated at normal temperature and pressure, so this technique best suit to thermo sensitive fruit juices. Hence OD is best alternative to concentrate fruit juices with best quality and low cost. [7].

Different operating factors, like feed and osmotic agent temperature, flow rate, initial concentration, and the membrane properties have effect on the water flux in OD process. Different studies are available in literature, which reveals the effect of all those factors on the performance of the OD process. However, all studies have discrepancy among them. And also little information has been published so far, in order to obtain the optimal operating conditions for practical implication of OD process in the food Industry.

Effect of all the operating factors is difficult to study using experiments as it is expensive and time consuming, therefore, in this research study mathematical modeling technique is used to study the effect of different operating parameters [5, 6].

2. MASS TRANSFER EQUATIONS

As the water transport is divided into three categories, similarly mass transfer will also be studied separately in three sections. The basic model equation for water transport is given by eq. (3.1) that relates mass flux (J_w) to the driving force, i-e vapour pressure difference at both liquid-vapour interfaces of the membrane (ΔP_w^m), also membrane proportionality coefficient (K_m) which is also called membrane permeability is used in model flux equation as membrane mass transfer coefficient.

$$J_w = K_m(\Delta P_{w,m}) \dots \dots \dots (3.1)$$

Since it is difficult to calculate ($\Delta P_{w,m}$) because it depends on membrane surface temperature and solute concentrations which are not always accessible. So another approach can be used to calculate the flux is given by equation 3.2

$$J_w = K(\Delta P_{w,bulk}) \dots \dots \dots (3.2)$$



$$K = \left(\frac{1}{K_f}\right) + \left(\frac{1}{K_m}\right) + \left(\frac{1}{K_p}\right) \dots \dots \dots (3.3)$$

2.1 Feed Side Mass Transfer Coefficient

As the Feed is flowing inside fibre (tube side), the mass transfer coefficient can be calculated using mass transfer analogy for laminar flow inside a pipe, i-e the Sieder-Tate equation (Geankoplis, 1983 & 1993;Heldman & Singh, 1981).

$$K_f = 1.886 \left(Re.Sc.\frac{d_h}{L} \right)^{\frac{1}{3}} . D_{AB}/d_h \dots \dots \dots (3.4)$$

$$Sh = k.\frac{d_h}{D_{AB}}, \quad Re = \rho v d_h/\mu, \quad Sc = \mu/\rho D_{AB}$$

2.2 Membrane Mass Transfer Coefficient

When the membrane pore diameter is less than mean molecular diameter, then the molecules tends to collide with the walls of membrane pore walls this type of diffusion is called Knudsen diffusion. And similarly when membrane pore diameter is greater than mean molecular diameter, then the molecules collide more frequently within themselves, and that type of diffusion is called molecular diffusion [12].

For both the mechanisms membrane Mass transfer Coefficient is given in equation (3.5) & (3.6), respectively.

$$K_m^K = \frac{M_w}{RT} \left(\frac{2}{3}\right) \left(\frac{\epsilon r}{X\delta}\right) \sqrt{\frac{8RT}{\pi M_w}} \dots \dots \dots (3.5)$$

$$K_m^M = \frac{M_w \epsilon D_w a}{RT X\delta} \frac{P}{(P_a)} \dots \dots \dots (3.6)$$

In order to know which of the following two mechanisms will be predominant, Knudsen number(K_n) is a criterion;

Knudsen number is the ratio of mean molecular free path (λ) of the diffusing molecular to the mean pore diameter of the membrane, and is given by the eq (3.7).

$$K_n = \frac{\lambda}{2r} \quad \lambda = \frac{3.2\mu}{P} \sqrt{\frac{RT}{2\pi M}} \dots \dots \dots (3.7)$$

If $K_n > 10$ then Knudsen diffusion mechanism will be dominant, if $K_n < 1/100$ the molecular diffusion mechanism is dominant, or if the value of K_n is in between, then the diffusion is in transition regime [8, 9].

For the current study, $K_n < 1/100$ means that molecular diffusion mechanism is dominated.

2.3 Permeate Side Mass Transfer Coefficient

It is studied that packing density also has large effect of Reynolds number and hence mass transfer coefficient. Studies on shell side mass transfer suggested that Sherwood number depends on fibre packing densities Φ [50].

In this research work different correlations were used, best results were obtained using correlation proposed by Costello et al. 1993 was chosen also constraints were same as our experimental conditions [9].

The correlation is as follows:

$$Sh = (0.53 - 0.58\phi) Re^{0.53} Sc^{0.33} \dots \dots \dots (3.8)$$



$$kos = \frac{D_{AB}}{d_s} (0.53 - 0.58\phi) Re^{0.53} Sc^{0.33} \dots\dots (3.9)$$

3. Model Algorithm

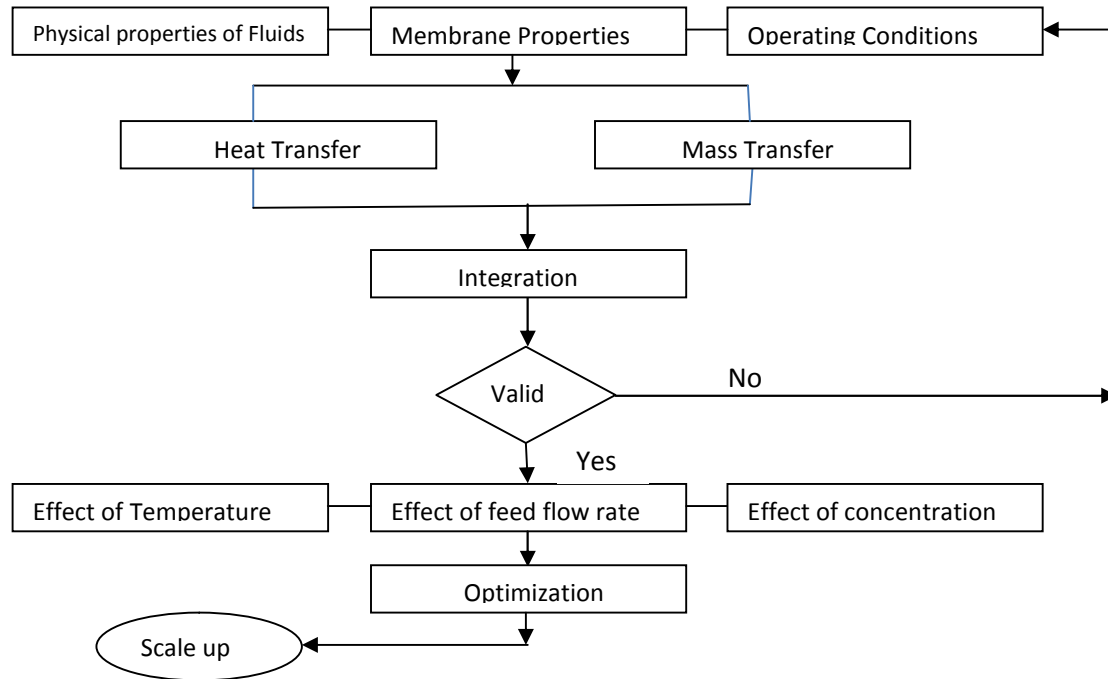


Figure 1 Model Algorithm for Osmotic membrane distillation for fruit juice concentration

4. RESULTS AND DISCUSSIONS

4.1. Model validation

Model was validated using experimental data from literature. H. Valdes *et al* performed experiments using hollow fiber membrane module having same number of fibers and materials of construction as in current studies. Experiments were performed by circulating feed and osmotic agents through hollow fiber membrane contactor at specified operating conditions. Feed and osmotic flow rates were adjusted between 0.1 and 1.0 Lmin⁻¹ and calcium chloride was used as osmotic agent. Results suggested that by varying flow rates, flux obtained was from 0.35 up to 0.48 kg h⁻¹.m⁻². In current study mathematical modeling was performed on hollow fiber membrane module, using same conditions as used in literature the results obtained by varying flow rates from 0.1 to 1.0 Lmin⁻¹ as shown in Figure 2.

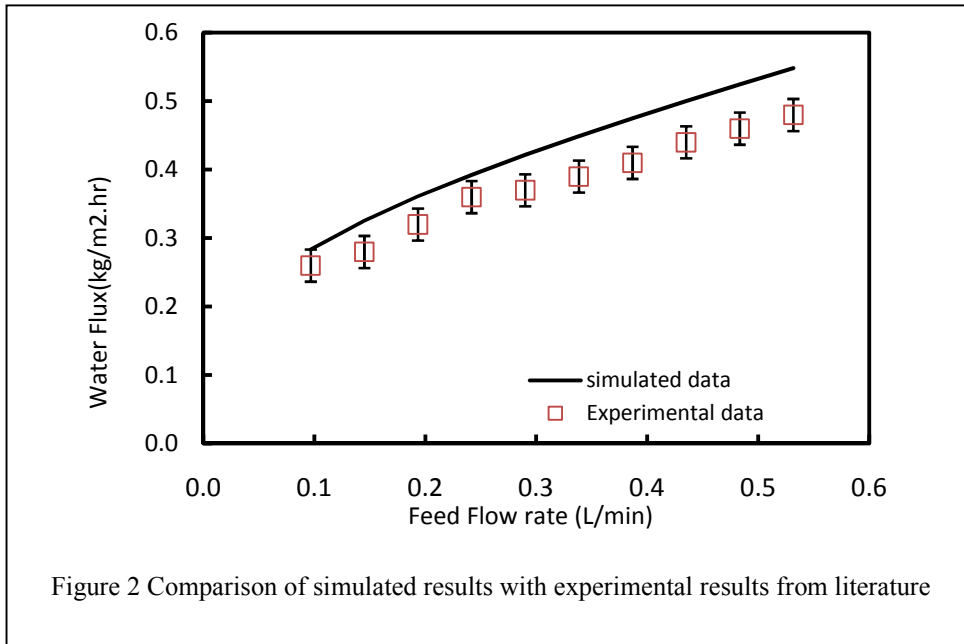


Figure 2 Comparison of simulated results with experimental results from literature

4.2. Effect of Osmotic agent Concentration

Effect of Osmotic concentration was studied by varying its value was varied from 1M to 5M. By increasing the concentration of osmotic agent (CaCl₂) from 1M to 5M, water flux was increased from 0.2 kgm⁻².h⁻¹ to 3.5kgm⁻².h⁻¹ due to increase in driving force for mass transfer. Higher concentration of CaCl₂ means that vapor pressure at the permeate side is lower than the vapor pressure at the feed side and water vapours rapidly transfers through the membrane pores to the permeate side. The effect of Osmotic solution concentration on water flux is given in Figure 4.

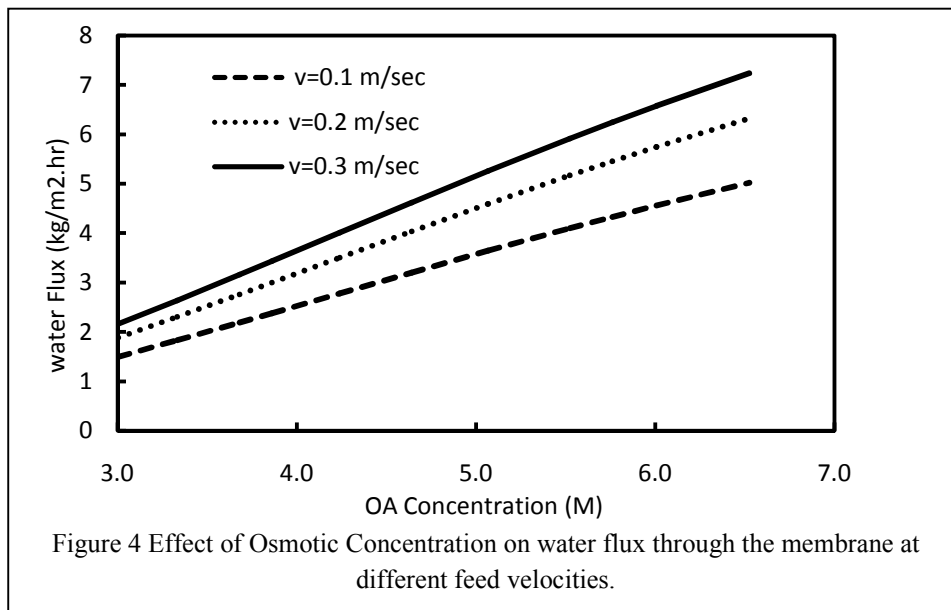
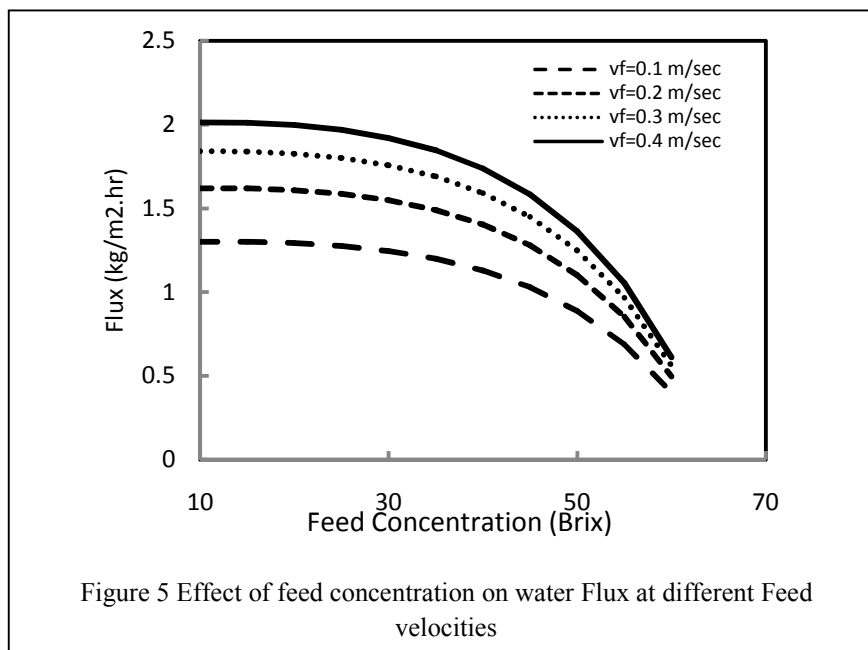


Figure 4 Effect of Osmotic Concentration on water flux through the membrane at different feed velocities.

4.3. Effect of Feed concentration on water flux

The effect of feed concentration was then studied for different feed velocities and it was observed that water flux is higher in case of high feed velocity. It is mainly due to fact that high velocity corresponds to high Reynolds number. And at high Reynolds number effect of concentration polarization is less, due to which flux is high.

The effect was then studied at different feed velocities. Keeping feed velocity at 0.1 m/sec, osmotic agent velocity at 0.2 m/sec and osmotic agent concentration was kept at 4M. Bulk temperature at feed and osmotic side was kept at 298K. By increasing feed concentration from 10°Brix to 60°Brix, flux declined from 0.7 Kg^m⁻².h⁻¹ to 0.5Kg^m⁻².h⁻¹. Similarly when the velocity was increased to 0.4m/sec, keeping other operating conditions constant, flux decline occurred from 2Kg^m⁻².h⁻¹ to 0.5Kg^m⁻².h⁻¹. Effect of Feed concentration on water flux is given in Fig.05.



In this research work, the effects of different operating parameters were studied theoretically, and the importance of operating parameters process performance was identified. In this study, a mathematical model was develop for the osmotic distillation process and several key parameters were studied, like feed and brine concentration, feed and brine velocities and their effect on water transport flux and overall mass transfer coefficient was also studied. OD fluxes obtained in this study ranged from 0.2kg.m⁻².h⁻¹ to 3.4 kg.m⁻².h⁻¹. It was observed that Flux as well as overall mass transfer coefficient increased with increase temperature as water vapours directly proportional to temperature as suggested by Antoine equation. Similarly the effect of feed concentration was also studied, as the feed concentration increased, flux decline occurred because of the activity coefficient of feed solution. Effect of polarization layers was not the part of this studied so flux decline due to concentration polarization and temperature polarization as suggested in literature was not taken into account for this study.

The water transport model was developed in this research using resistance in series method. The developed model successfully applied to calculate overall mass transfer coefficient in different zones. Then the water flux was calculated using vapour pressure difference and overall mass transfer coefficient.



REFERENCES

- [1] Courel M., Dornier M., Rios G.M., Reynes M., Modelling of water transport in osmotic distillation using asymmetric membrane, *Journal of Membrane Science* 173 (2000) 107–122.
- [2] Alves V.D., Coelhoso I.M., Mass transfer in osmotic evaporation: effect of process parameters, *Journal of Membrane Science* 208 (2002) 171–179.
- [3] Courel M., Dornier M., Herry J.M., Rios G.M., Reynes M., Effect of operating conditions on water transport during the concentration of sucrose solutions by osmotic distillation, *Journal of Membrane Science* 170 (2000) 281–288.
- [4] Alves V.D., Coelhoso I.M., Orange juice concentration by osmotic evaporation and membrane distillation: a comparative study, *J. Food Eng.* 74 (2006) 125-134.
- [5] Carlo Gostoli, Thermal effects in osmotic distillation, *Journal of Membrane Science* 163 (1999) 75–91.
- [6] Naveen Nagaraj , GanapathiPatil, B. RavindraBabu , Umesh H. Hebbar , K.S.M.S. Raghavarao , Sanjay Neneb, Mass transfer in osmotic membrane distillation, *Journal of Membrane Science* 268 (2006) 48–56.
- [7] Alves V.D., Coelhoso I.M., Effect of membrane characteristics on mass and heat transfer in the osmotic evaporation process, *Journal of Membrane Science* 228 (2004) 159-171.
- [8] Mengual J.I., Ortiz de Z'arate J.M., Pe'na L., Vel'azquez A., Osmotic distillation through porous hydrophobic membranes, *Journal of Membrane Science* 82 (1993) 129–140.
- [9] RavindraBabu B., Rastogi N.K., Raghavarao K.S.M.S., Mass transfer in osmotic membrane distillation of phycocyanin colorant and sweet-lime juice, *Journal of Membrane Science* 272 (2006) 58–69.
- [10] Alves V.D., Coelhoso I.M., Orange juice concentration by osmotic evaporation and membrane distillation: A comparative study, *Journal of Food Engineering* 74 (2006) 125–133.
- [11] Thanedgunbaworn R., Jiraratananon R., Nguyen M.H., Shell-side mass transfer of hollow fibre modules in osmotic distillation process, *Journal of Membrane Science* 290 (2007) 105–113.
- [12] Alves V.D., Coelhoso I.M., Mass transfer in osmotic evaporation: effect of process parameters, *Journal of Membrane Science* 208 (2002) 171–179.



Conference Proceedings SPI 2014 [63-72]

Simulation of HFMC for Heavy Metal (Cu) Extraction With Chelating Extractants

Iftikhar Ahmed¹, Dr. Muhammad Younas²

^{1,2}Department of Chemical Engineering, University of Engineering and Technology Peshawar, Pakistan.

¹iftikhar.371@gmail.com, ²engr_unas@nwfpuet.edu.pk

Abstract:

In the current study recovery of copper (II) from aqueous waste streams has been studied theoretically through hollow fiber membrane contactor. Copper (II) reacted with an organic extractant Trifluoroacetylacetone (TFA) at the membrane interface and thus copper complex molecules was transferred from one side of membrane to other side of membrane. Mathematical model describing mass transfer phenomena, Poiseuille flow and design equations were integrated. The integrated process model algorithm was scripted in MATLAB® 8.1.2. The model analysis incorporate reaction kinetics of the copper with extractant, conservation rate equation of copper ion and extractant incorporating transfer of copper across the membrane pore as depicted by Fick's law of diffusion. Simulations have been performed for a wide range of different operating conditions in order to determine the optimum set of conditions for a particular operation. The model results were found to be in good agreement with the experimental work available in literature. It was found that the model predicted the data reasonably well, proving the model to be a useful tool for evaluating the potential applications of the technology.

Keywords: HFMC, Copper extraction, Simulation, Modelling

1. INTRODUCTION

Copper is becoming a vital metal due to continuous rise in its demand for circuit boards in microelectronics industry, electro refining industry, mining waste and fertilizer industry. Effluents streams of mining and metal processing industries containing heavy metal is considered to be potential threat for environment. In most part of the world there are large reserves of copper mines which catch the attention of researchers to think about cost



effective and environment friendly process for the extraction. Therefore it is imperative to develop efficient techniques for copper (II) extraction [1].

The older techniques are tedious, lingering and are less efficient. It's need of time to replace these techniques with the commercialized membrane based separations. Environmental threats, paucity of water, and decreasing price of membranes also favor their use. In past few years, considerable effort has been made to recover the heavy metals from aqueous streams with the help of chelating extractants through hollow fibre membrane contactors [2].

A lot of literature work is available regarding the study of copper recovery using different types of extractant in numerous diluents. Two approaches are generally adopted for modelling the HFMCs. First approach emphasis on overall mass transfer coefficient (K) which is calculated from three resistances encountered in series. Second approach is based on the mass and momentum conservation equations along with associated boundary conditions. Bringas et al [3] published extensive work about mass transfer modelling in liquid membrane contactors. Bocquet et al. [4] presented a resistance-in-series model for extraction of ethanol by using the sub critical CO₂ or propane. M. Younas et al developed a modified axial-radial dynamic model for HFMC module [2]. Gonzglez-Mufioz et al [5] worked on extraction and stripping process in HFMC and developed a resistance-in-series model. The result obtained from the model match with the experimental results with the reasonable accuracy.

Some researchers [6, 7 & 8] modelled non-dispersive HFM based gas-liquid and LLE processes by using another approach i.e. by the development of conservation equations. Sherazian et al [7] employ the same approach to model the non-dispersive extraction of heavy metals. Their 2-D axial radial mass transfer model assumed axial-radial diffusion through MC. Yao et al [9] worked on the recovery of Cu (II) from aqueous solution by using LIX-84 in ELM. Additionally both the extracting and stripping occurred in one step.

2. Mass Transfer Modeling

2.1 Development of mathematical model

Membrane-based LLE is a concentration-driven operation and the transfer of the solute can be explained by Fick's law of diffusion. Solute transfer across the membrane occurred in the following steps as shown in the figure 1.

- The solute flows through the feed boundary layer, from the bulk phase to the interface.
- Crosses the feed/solvent interface.
- Diffuses in the pore filled with the solvent phase.
- Flows through the solvent boundary layer.

During this flow the solute encounters three resistances to the mass transfer.

- Resistance in the aqueous phase boundary layer
- Resistance in the membrane
- Resistance in the solvent phase boundary layer

The transport of the fluid from the aqueous boundary layer is given by

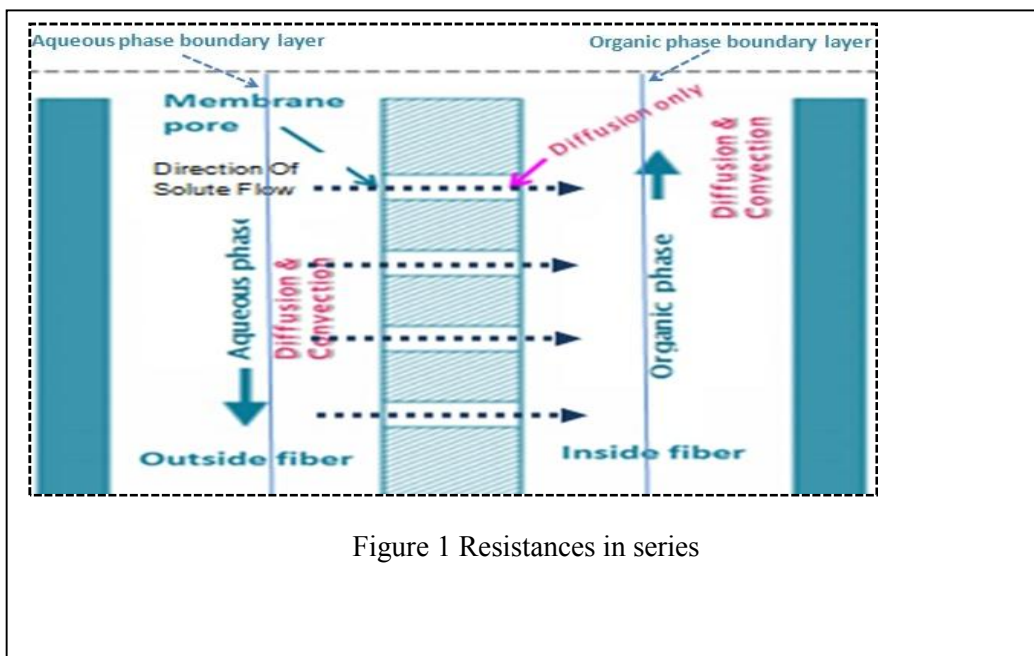


Figure 1 Resistances in series



$$m = k_{aq} A_{ext}(C_1^0 - C_2) \quad (1)$$

Flux through membrane is given by

$$k_{mb} A_{mb}(C_3 - C_4) \quad (2)$$

The reaction of Cu^{+2} with the chelating agent at the aqueous-organic interface to form the copper-complexant is given by many researchers [11] as



Similarly flux through solvent boundary layer is given by

$$m = k_{sol} A_{ext}(C_4 - C_5) \quad (4)$$

Applying the mass balance on solute in aqueous phase

$$m = Q_{aq}(C_1^0 - C_1^{eq}) \quad (5)$$

Applying the mass balance on copper-complex in organic phase

$$m = Q_{org}(C_5^{eq} - C_5^0) \quad (6)$$

The partition coefficient of a component is important parameter which defines the limit of extraction. It is the ratio of the component concentration in organic phase to component concentration in aqueous phase at equilibrium

$$P = \frac{(C_1^0 - C_1^{eq})}{C_1^0} \quad (7)$$

Following the resistance in series model, overall mass transfer coefficient based on aqueous phase when the aqueous phase is flowing on the shell side through a hydrophobic membrane is given by the following expression.

$$K_{sh} = \frac{1}{k_{aq}} + \frac{d_{ext}}{Pk_{mb}d_{lm}} + \frac{d_{ext}}{Pk_{org}d_{int}} \quad (8)$$

This equation were modified for the other configuration i.e. feed-fiber configuration. Similarly extraction efficiency is considered as the ratio of amount of copper transferred from aqueous phase to the organic phase to the



initial amount of copper in the aqueous phase. The integrated model developed by solving these equations predicts the overall mass transfer coefficient, extraction efficiency and the solute flux across the membrane. The simulation parameters are listed in table 2.

Table 1. Geometrical Characteristics of module

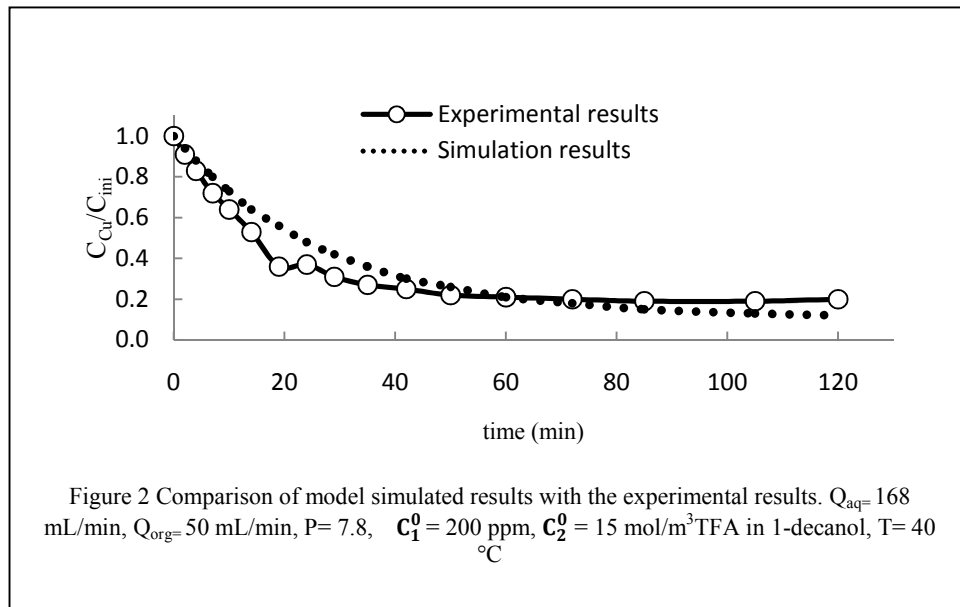
Geometrical Characteristics	Module X-50
Internal diameter of the fiber (m)	2.2×10^{-4}
External diameter of the fiber (m)	3×10^{-4}
Mean diameter of pore (m)	4×10^{-8}
Diameter of the flow-cell (m)	4.94×10^{-4}
Diameter of the module shell (m)	42.5×10^{-3}
Length of the module (m)	122×10^{-3}
Number of fibers	7400
Porosity (%)	40

Table 2. Simulation parameters

Simulation parameters	values
C_1^0 Copper(II)ppm,mole.m ⁻³	200-1000
C_2^0 extractant %v/v	15
Temperature, k	298
Q_{aq} , ml.min ⁻¹	300-1000
Q_{org} , ml.min ⁻¹	300-1000
V_{aq}	1 L
V_{org}	1 L

2.2 Model Validation

Current study deals with the model simulation of process for once-through mode of extraction of copper. While in the literature experimental data is reported for the extraction of copper (II) from aqueous phase with TFA extractant in HFMCs for recycled based process [12]. Therefore single-fiber steady-state model was modified to dynamic model and simulated for the HFMC Liqui-CelTM X-50 module. Additionally the flow is counter current to each other with the aqueous phase flowing through shell side of the membrane. Diffusion coefficient of copper (II) ions in aqueous phase and copper-T FA complex were calculated from Hayduk and Minhas correlation [13]. The mass transfer correlations were estimated by using the correlations as proposed by Prasad and Sirkar [14]. Flow rates and pressure drops were kept constant. Overall the simulated results were found to be in good agreement with the experimental results with $\pm 5\%$ tolerable experimental error. Additionally it can be observed that decrease in concentration is rapid up to 60 minute extraction but it become progressively slow towards the end of process.

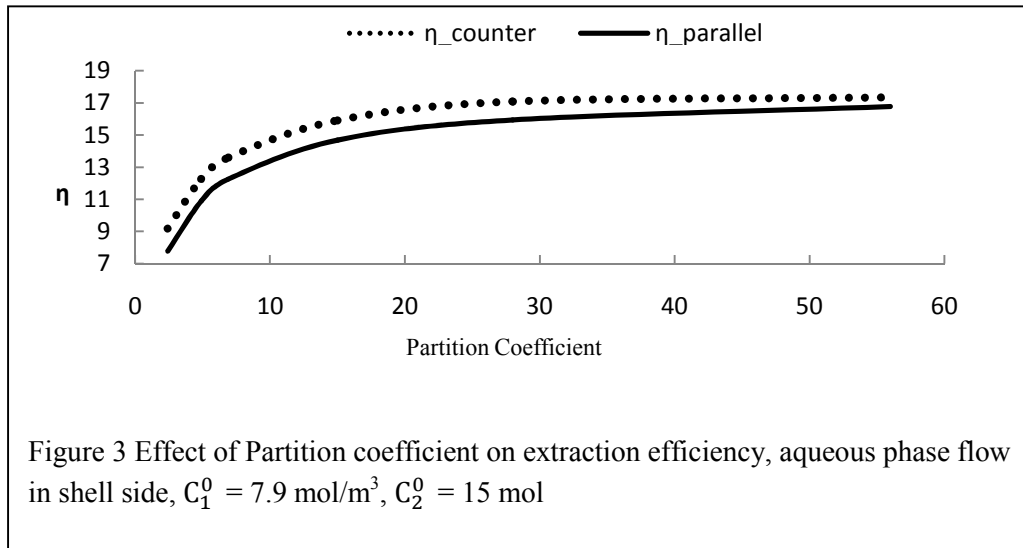


3. EFFECT OF DIFFERENT VARIABLES

Once the model has been validated simulation were performed to explore the influence of various operating parameter and hydrodynamic conditions.

3.1 Effect of partition coefficient

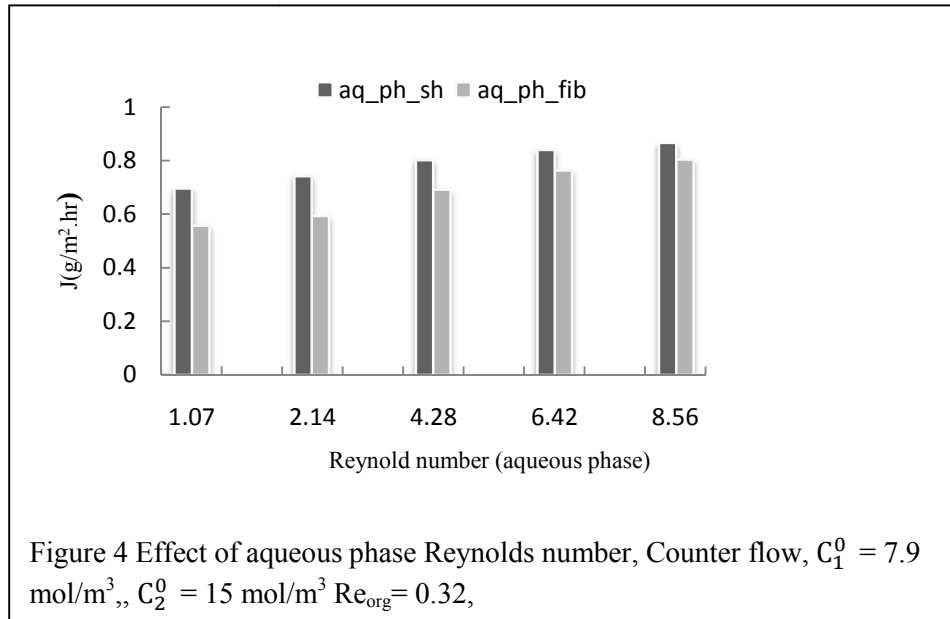
Interest has been taken to take into account the effect of partition coefficient on the liquid-liquid extraction of copper in HFMC. Simulation were performed at the 2.4, 4.9,6.9,15 and 28, the arbitrary value of partition coefficient at aqueous and organic phase flow rate of 300 mL/min with initial concentration of copper at 7.9 mole/m³. From figure 3 it can be seen that extraction efficiency enhanced at the higher value of partition coefficient. It can also be concluded that initially increase in extraction efficiency is rapid, but the extraction progressively becomes stable at the higher values of partition coefficient. Furthermore it can be observed that in every case extraction is best performing when aqueous and organic phase are rotated counter currently to each other. Flux also showed the same trend.



3.2 Effect of Hydrodynamics Conditions

Simulation was performed to analyse the effect of different aqueous and organic phase flow rate at the initial copper concentration of 7.9 mol/m^3 with TFA concentration of 15 mole/m^3 . Aqueous phase flow rates were 1.67×10^{-6} , 3.33×10^{-6} , 6.67×10^{-6} , 1×10^{-5} , and 1.33×10^{-5} and $1.67 \times 10^{-5} \text{ m}^3/\text{sec}$. The corresponding values of Reynolds number for these flow rates are 1.07, 2.14, 4.28, 6.42, 8.6 and 10.70. The organic phase flow rate is constant at $5 \times 10^{-6} \text{ m}^3/\text{sec}$; the corresponding Reynolds number for this flow rate is 0.32. From the figure 4 it can be seen that improved value of flux obtained at higher value of aqueous phase flow rate, furthermore within the given Reynolds number the extraction is enhanced when the aqueous phase flows through shell side of module.

Younas et al [15] studied the extraction of aroma compound dimethyletrisulfide DMTS and 2-phenyl ethanol in module X-40. Their results showed that extraction enhanced for high flow rate of aqueous phase for dimethyletrisulfide, while in the case of 2- phenyl ethanol negligible change in extraction efficiency has been shown. Viladomat et al [16] investigated the extraction of DMDS (dimethyldisulfide) for the two aqueous phase flow rate (shell side) and same results were obtained. Pierre et al. [17] and [18] explored the recovery of aroma compounds DMTS and MTB (S-methyl thiobutanoate) by hexane, the same trends has been observed in their work except for PE which has the partition coefficient less than 1.



3.3 Other factor to be considered

There are some other variable which influence the extraction. Simulation has been done to cover the whole spectrum of variable. It has been found the increase in porosity to tortuosity ratio of the fibers the increases the efficiency. Flux shows the same trend as the efficiency, as the ratio increases, more area or passage becomes available for the solute to cross the membrane resulting in higher flux. Length of the fiber is another influencing parameter; in this regard the results shown that at the longer fiber tends to enhanced the extraction efficiency but at the cost of reduced flux. Another interesting trend has been observed when internal and external diameter simultaneously changed but keeping the thickness constant. Most efficient extraction was found with the internal and external diameter of 0.00022m and 0.0003m respectively. Two feed flow configuration i.e. the feed flowing inside the shell and feed flowing inside the fiber has also been investigated when testing the each factors. It can easily be figure out that extraction is well performing when feed is routed through shell side. This trend can be attributed to larger interfacial area offered by shell compartment of HFMC.

4. CONCLUSION

Liquid-liquid extraction of copper with Trifluoro-acetylacetone (TFA) in hydrophobic membrane contactor was studied theoretically. A mass transfer model was developed and validated with the experimental results. The simulation was run to explore the influence different variable on extraction of copper. The following results were obtained.



- It was found that 2000 fiber with the same dimension give highest flux and mass transfer coefficient, but maximum efficiency was found with 7400 fiber.
- Extraction has been found to be well performing when feed is routed through shell side rather than the fiber side of the module.
- Higher efficiency is obtained when the aqueous and organic phase circulated counter current to one another rather than parallel contact.
- Partition coefficient was found as most influencing parameter; higher extraction was obtained at the higher value of partition coefficient but up to a certain limit after that effect become negligible.
- With the increase in Reynolds's number of aqueous feed improved value of flux obtained.
- Increase in external diameter keeping the internal diameter constant lead to increase thickness of the membrane which ultimately reduced flux.
- Increase in porosity/tortuosity of membrane higher flux is obtained with the slightly better efficiency
- Longer fiber tends to enhance the extraction efficiency but at the cost of reduced flux.

References

- [1] M. Younas, "Dynamic Modelling Of Membrane Contactors For Liquid-Liquid Extraction: Experimentation And Simulation PhD thesis " Institut Européen des Membranes Université de Montpellier 2. (2011): 9-10.
- [2] M. Younas, S. Druon-Bocquet, and J. Sanchez. "Kinetic and Dynamic Study of Liquid-Liquid Extraction of Copper in a HFMC: Experimentation, Modeling, and Simulation" American Institute of Chemical Engineers AIChE J, 56: 1469–1480, 2010.
- [3] Bringas, E., San Rom, MF., Irabien, JA., and Ortiz, I. "An overview of the mathematical modeling of liquid membrane separation processes in hollow fibre contactors." *J. Chem. Technol. Biotechnology*, 84 (2009): 1583–1614.
- [4] Bocquet S., Romero, J., Sanchez J., Rios, G.M. "Membrane contactors for the extraction process with subcritical carbon dioxide or propane: simulation of the influence of operating parameters." *Journal of Supercritical Fluids* 41.2 (2007): 246–256.
- [5] Gonzglez-Mufioz, M.J., Luque, S, Alvarez, J.R, Coca, J. "Simulation of integrated extraction and stripping processes using membrane contactors." *Desalination* 163 (2004): 1-12.
- [6] Marjani, A., Shirazian, S. "Simulation of heavy metal extraction in membrane contactors using computational fluid dynamics." *Desalination* 281 (2011): 422–428.
- [7] Fadaei F., Shirazian, S., Ashrafzadeh, S.N. "Mass transfer simulation of solvent extraction in hollow-fiber membrane contactors." *Desalination* 275 (2011): 126–132.
- [8] Marjani, A., Shirazian, S. "CFD Simulation of SO₂ Removal from gas Mixtures using Ceramic Membranes." *World Academy of Sci., Engg. and Tech.* 58 (2011): 868-871.
- [9] Shih-Yao, Hu, B., Wienczek, J.M. "Emulsion-liquid-membrane extraction of copper using a hollow-fiber contactor." *AIChE J* 44 (1998): 570-581.
- [10] S. Bocquet, F.G. Viladomat, C. Muvdi Nova, Sanchez, V. Athes, I. Souchon. "Membrane-based solvent extraction of aroma compounds: Choice of configurations of hollow fiber modules based on experiments and simulation." *J. Membrane. Sci.* 281 (2006): 358 - 368.
- [11] Carter, Stephen P., and Henry Freiser. "Kinetics and mechanism of the extraction of copper with 2-hydroxy-5-nonylbenzophenone oxime." *Analytical Chemistry* 52.3 (1980): 511-514.
- [12] Younas, Mohammad, Stéphanie Druon-Bocquet, and José Sanchez. "Experimental and theoretical mass transfer transient analysis of copper extraction using hollow fiber membrane contactors." *Journal of Membrane Science* 382.1 (2011): 70-81



- [13] B.E. Poling, J.M. Prausnitz, J.P. O'Connell, *The properties of gases and liquids*, 5th edn, McGraw-Hill, New York, 2001.
- [14] Prasad, Ravi, and K. K. Sirkar. "Dispersion-free solvent extraction with microporous hollow-fiber modules." *AIChE Journal* 34.2 (1988): 177-188.
- [15] Carter, Stephen P., and Henry Freiser. "Kinetics and mechanism of the extraction of copper with 2-hydroxy-5-nonylbenzophenone oxime." *Analytical Chemistry* 52.3 (1980): 511-514.
- [16] Viladomat, Fabrice Gascons, et al. "Liquid-liquid and liquid-gas extraction of aroma compounds with hollow fibers." *AIChE. J* 52.6 (2006): 2079-2088.
- [17] Pierre, François-Xavire, et al. "Membrane-based solvent extraction of sulfur aroma compounds: influence of operating conditions on mass transfer coefficients in a hollow fiber contactor." *Desalination* 148.1 (2002): 199-204.
- [18] Pierre, F. X., I. Souchon, and M. Marin. "Recovery of sulfur aroma compounds using membrane-based solvent extraction." *Journal of Membrane Science* 187.1 (2001): 239-253.